Pontifícia Universidade Católica
do Rio de Janeiro

Raphael de Marreiros Cordeiro Machado

Domino tilings of 3-dimensional cylinders

Tese de Doutorado

Thesis presented to the Programa de Pós-graduação em Matemática of PUC-Rio in partial fulfillment of the requirements for the degree of Doutor em Matemática.

Advisor: Prof. Nicolau Corção Saldanha
Co-advisor: Prof. Caroline Jane Klivans

Rio de Janeiro
February 2025

Pontifícia Universidade Católica
do Rio de Janeiro

Raphael de Marreiros Cordeiro Machado

Domino tilings of 3-dimensional cylinders

Thesis presented to the Programa de Pós-graduação em Matemática of PUC-Rio in partial fulfillment of the requirements for the degree of Doutor em Matemática. Approved by the Examination Committee.

Prof. Nicolau Corção Saldanha
Advisor
Departamento de Matemática – PUC-Rio

Prof. Caroline Jane Klivans
Co-advisor
Division of Applied Mathematics – Brown University

Prof. Carlos Tomei
Departamento de Matemática – PUC-Rio

Prof. Catherine Wolfram
Department of Mathematics – Yale University

Prof. Leonardo Henrique Caldeira Pires Ferrari
Mathematical Institute of the Polish Academy of Sciences – IMPAN

Prof. Robert David Morris
Instituto Nacional de Matemática Pura e Aplicada – IMPA

Prof. Simon Griffiths
Departamento de Matemática – PUC-Rio

Prof. Yoshiharu Kohayakawa
Departamento de Ciência da Computação – USP

Rio de Janeiro, February 17th, 2025

Raphael de Marreiros Cordeiro Machado

Bachelor's in Mathematics from Universidade Federal Fluminense (UFF), 2018. Master's in Mathematics from Pontifícia Universidade Católica do Rio de Janeiro (PUC-Rio), 2021.

Bibliographic data

Machado, Raphael de Marreiros Cordeiro

Domino tilings of 3-dimensional cylinders / Raphael de Marreiros Cordeiro Machado ; advisor: Nicolau Corção Saldanha ; co-advisor: Caroline Jane Klivans. – 2025.
59 f. : il. color. ; 30 cm

Tese (doutorado)– Pontifícia Universidade Católica do Rio de Janeiro, Departamento de Matemática, 2025.
Inclui bibliografia

1. Matemática – Teses. 2. Coberturas tridimensionais. 3. Dominós. 4. Movimentos locais. 5. Flips. 6. Componentes conexas por flips. I. Saldanha, Nicolau Corção. II. Klivans, Caroline Jane. III. Pontifícia Universidade Católica do Rio de Janeiro. Departamento de Matemática. IV. Título.

CDD: 510

Acknowledgments

To my advisor, Prof. Nicolau Saldanha, for his guidance and encouragement throughout this work.

To Prof. Caroline Klivans, for her availability and generous hospitality during my stay at Brown University.

To my family and friends.

To CAPES, PUC-Rio and Brown University for their support.

This study was financed in part by the Coordenação de Aperfeiçoamento de Pessoal de Nível Superior - Brasil (CAPES) - Finance Code 001

Abstract

Machado, Raphael de Marreiros Cordeiro; Saldanha, Nicolau Corção (Advisor); Klivans, Caroline Jane (Co-Advisor). **Domino tilings of 3-dimensional cylinders**. Rio de Janeiro, 2025. 59p. Tese de Doutorado – Departamento de Matemática, Pontifícia Universidade Católica do Rio de Janeiro.

We consider three-dimensional domino tilings of cylinders $\mathcal{D} \times [0, N]$, where $\mathcal{D} \subset \mathbb{R}^2$ is a fixed quadriculated disk and $N \in \mathbb{N}$. A domino is a $2 \times 1 \times 1$ brick. A flip is a local move in the space of tilings $\mathcal{T}(\mathcal{D} \times [0, N])$: two adjacent and parallel dominoes are removed and then placed in a different position. The twist is a flip invariant which associates an integer number to each tiling. For certain disks $\mathcal{D}$, called *regular*, any two tilings of $\mathcal{D} \times [0, N]$ sharing the same twist can be connected through a sequence of flips when extra vertical space is added to the cylinder. We prove that the absence of a bottleneck in a hamiltonian disk implies regularity. Conversely, we show that the presence of a bottleneck in a disk $\mathcal{D}$ often indicates irregularity. In many cases, we further demonstrate that $\mathcal{D}$ belongs to a specific class of irregular disks, which we define as *strongly irregular*. Furthermore, for any strongly irregular disk $\mathcal{D}$, we prove that the connected components under flips consist of exponentially small fractions of $\mathcal{T}(\mathcal{D} \times [0, N])$.

Keywords

Three-dimensional tilings; Dominoes; Local moves; Flips; Connected components under flips.

Resumo

Machado, Raphael de Marreiros Cordeiro; Saldanha, Nicolau Corção; Klivans, Caroline Jane. **Coberturas por dominós de cilindros tridimensionais**. Rio de Janeiro, 2025. 59p. Tese de Doutorado – Departamento de Matemática, Pontifícia Universidade Católica do Rio de Janeiro.

Consideramos coberturas por dominós de cilindros tridimensionais da forma $\mathcal{D} \times [0, N]$, onde $\mathcal{D} \subset \mathbb{R}^2$ é um disco quadriculado fixo e $N \in \mathbb{N}$. Um dominó é um paralelepípedo $2 \times 1 \times 1$. Um flip é um movimento local no espaço de coberturas $\mathcal{T}(\mathcal{D} \times [0, N])$: dois dominós adjacentes e paralelos são removidos e colocados em uma posição diferente. O twist é um invariante por flips que associa um número inteiro a cada cobertura. Para certos discos, chamados *regulares*, quaisquer duas coberturas de $\mathcal{D} \times [0, N]$ que compartilham o mesmo twist podem ser conectadas por uma sequência de flips quando espaço vertical é adicionado ao cilindro. Provamos que a ausência de gargalos em um disco hamiltoniano implica regularidade. Reciprocamente, mostramos que a presença de gargalos em um disco $\mathcal{D}$ geralmente indica irregularidade. Em muitos casos, demonstramos ainda que $\mathcal{D}$ pertence a uma classe específica de discos irregulares, que definimos como *fortemente irregulares*. Além disso, para qualquer disco fortemente irregular $\mathcal{D}$, provamos que as componentes conexas por flips consistem de frações exponencialmente pequenas de $\mathcal{T}(\mathcal{D} \times [0, N])$.

Palavras-chave

Coberturas tridimensionais; Dominós; Movimentos locais; Flips; Componentes conexas por flips.

Table of contents

1
Introduction

Problems involving domino tilings have been widely studied, particularly due to their connections with topics such as dimer models and perfect matchings. The study of domino tilings originated in two dimensions, where a region refers to a finite connected union of closed unit squares with vertices in $\mathbb{Z}^2$. In this scenario, a *domino* is a rectangle with sides of length one and two, formed by the union of two adjacent closed unit squares. A *domino tiling* of a region is a covering of the region by dominoes with disjoint interiors. Figure 1.1 illustrates examples of domino tilings of planar regions.

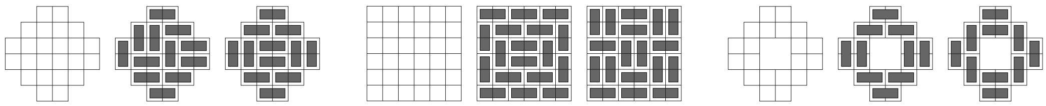

Figure 1.1: Three planar regions and two domino tilings of each.

Numerous significant results are known for two-dimensional domino tilings. Kasteleyn [10] demonstrated a connection between the number of domino tilings of a region and the Pffafian of a skew-symmetric matrix, as a consequence, the exact number of domino tilings of a $m \times n$ rectangle is derived. Independently, Temperley and Fisher [24] reached the same conclusion using a different method. Thurston [25] used arguments from combinatorial group theory, originally developed by Conway and Lagarias [6], to establish a criterion to decide whether a region admits a tiling. From a probabilistic perspective, random tilings have been explored to obtain properties of a typical domino tiling of a large region. Jockusch, Propp and Shor [9] investigated random tilings of regions called Aztec diamonds and proved the celebrated Artic Circle Theorem. Cohn, Elkies and Propp [4] later provided a new proof of this result. For more general regions, Cohn, Kenyon and Propp [5] showed that the behavior of random tilings is determined by a variational principle.

We are particularly interested in the problem of connectivity of domino tilings via local moves. A *flip* is a local move involving two dominoes: two adjacent and parallel dominoes are removed and placed in a different position after a 90° rotation. The flip connectivity problem consists in characterizing the connected components under flips of the space of tilings of a given region.

Thurston [25] proved that any two tilings of a *quadriculated disk* (i.e., a planar region homeomorphic to a closed disk) can be joined by a sequence of flips. Saldanha, Tomei, Casarin and Romualdo [23] showed, for planar non-simply-connected regions, the existence of a flip invariant called flux. Moreover, it is also proved that two domino tilings can be joined by a sequence of flips if and only if they have the same flux. For example, in Figure 1.1, the tilings of the disks can be connected through flips, unlike the tilings of the non-simply-connected region.

Domino tilings, along with the questions previously discussed, can be easily generalized to higher dimensions. However, the arguments used in two dimensions do not extend straightforwardly and much less is known, even for "well-behaved" regions. We focus on dimension three, where a region is a union of closed unit cubes and a *(3D) domino* is a parallelepiped formed by two closed unit cubes sharing a face.

Recently, Chandgotia, Sheffield and Wolfram [3] developed new tools to extend the results in [5] to 3D domino tilings. In a different vein, the transition of dimensions can drastically change the a priori expected result. For instance, Pak and Yang [20] showed that the counting tiling problem becomes computationally more complex in dimension three. Similarly, as we shall see, the space of tilings of a contractible 3D region is not necessarily flip connected.

In the last decade, significant progresses have been made on the flip connectivity problem, particularly in regions like cylinders [8, 13, 19, 22]. A three-dimensional *cylinder* $\mathcal{R}_N \subset \mathbb{R}^3$ is a cubiculated region formed by the cartesian product of a quadriculated disk $\mathcal{D}$ and an interval $[0, N]$ with $N \in \mathbb{N}$. The set of tilings of $\mathcal{R}_N$ is denoted by $\mathcal{T}(\mathcal{R}_N)$.

We adopt the approach used in [19] and draw a tiling of $\mathcal{R}_N$ by describing its behavior at each floor $\mathcal{D}\times[K-1, K]$; for instance, see Figure 1.2. Specifically, we depict a tiling as follows. We first fix the x-axis and the y-axis, the floors are then exhibited in increasing order from the left to the right. A domino parallel to either the x-axis or the y-axis, called a *horizontal domino*, is drawn as a planar domino. A domino parallel to the z-axis, called a *vertical domino*, is represented by two unit squares contained in adjacent floors, corresponding to its lower and upper halves. To avoid confusion, the upper half, which appears on the right-hand side, is left unfilled.

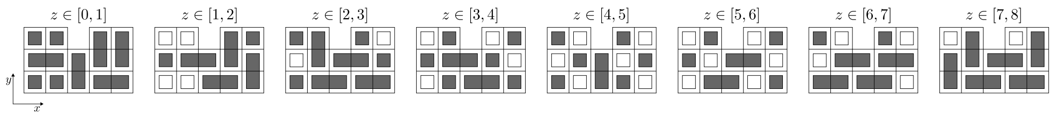

Figure 1.2: A tiling of a cylinder $\mathcal{D} \times [0, 8]$.

In general, we consider cylinders where the underlying disk is balanced and nontrivial. A disk $\mathcal{D}$ is *balanced* if it contains an equal number of black and white unit squares; a unit square $[a, a+1] \times [b, b+1] \subset \mathcal{D}$ with $(a, b) \in \mathbb{Z}^2$ is *white* if $a + b$ is even and *black* if $a + b$ is odd. Additionally, $\mathcal{D}$ is *trivial* if its unit squares are each adjacent to at most other two unit squares; for examples of trivial disks see Figure 1.3 below. It is not difficult to show that any two tilings of $\mathcal{D} \times [0, N]$ can be joined by a sequence of flips if $\mathcal{D}$ is trivial. However, the discussion is much more subtle for nontrivial disks.

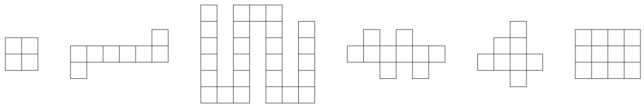

Figure 1.3: Six balanced quadriculated disks, the first three are trivial and the last three are nontrivial.

Milet and Saldanha [18] introduced the *twist* of a tiling for a large class of contractible cubiculated regions contained in $\mathbb{R}^3$. In this case, the twist is a flip invariant assuming values in $\mathbb{Z}$: given a tiling $\mathbf{t}$ of a suitable region, we have an integer $\mathrm{Tw}(\mathbf{t})$. The twist is defined by a combinatorial formula that counts certain pairs of dominoes oriented in different directions, in some sense measuring how twisted a tiling is. This definition is presented in Section 2.3.

The twist is closely related to the Hopf number, an invariant studied in physics whose existence is linked to the nontriviality of the third homotopy group of the sphere $\pi_3(S^2) = \mathbb{Z}$; for details, see [2, 7]. For regions more general than cylinders, which are not necessarily contractible, Freire, Klivans, Saldanha and Milet [8] provided a definition of the twist using homology theory. More recently, Khesin and Saldanha [12] presented an interpretation of the twist of a tiling as the relative helicity of a vector field.

In order to study the problem of connectivity by flips of the space of tilings of cylinders, we consider two distinct but related equivalence relations. Let $\mathcal{D}$ be a disk and consider tilings $\mathbf{t}_1 \in \mathcal{T}(\mathcal{R}_{N_1})$ and $\mathbf{t}_2 \in \mathcal{T}(\mathcal{R}_{N_2})$. We write $\mathbf{t}_1 \approx \mathbf{t}_2$ if $N_1 = N_2$ and there exists a sequence of flips joining $\mathbf{t}_1$ and $\mathbf{t}_2$. The $\approx$-equivalence classes are called connected components under flips.

We need two concepts to define the second equivalence relation. First, let *concatenation* $\mathbf{t}_1 * \mathbf{t}_2$ be the tiling of $\mathcal{R}_{N_1+N_2}$ formed by the union of $\mathbf{t}_1$ and the translation of $\mathbf{t}_2$ by $(0, 0, N_1)$. Second, for $N \in 2\mathbb{N}$ let the *vertical tiling* $\mathbf{t}_{\mathrm{vert},N} \in \mathcal{T}(\mathcal{R}_N)$ be the tiling consisting solely of vertical dominoes. We write $\mathbf{t}_1 \sim \mathbf{t}_2$ if $N_1 \equiv N_2 \pmod 2$ and there exist $M_1, M_2 \in 2\mathbb{N}$ such that $\mathbf{t}_1 * \mathbf{t}_{\mathrm{vert},M_1} \approx \mathbf{t}_2 * \mathbf{t}_{\mathrm{vert},M_2}$. Notice that if $\mathbf{t}_1 \not\sim \mathbf{t}_2$ then $\mathbf{t}_1 \not\approx \mathbf{t}_2$. However, as in Figure 1.4, there are cases where $N_1 = N_2$ and $\mathbf{t}_1 \sim \mathbf{t}_2$, while $\mathbf{t}_1 \not\approx \mathbf{t}_2$.

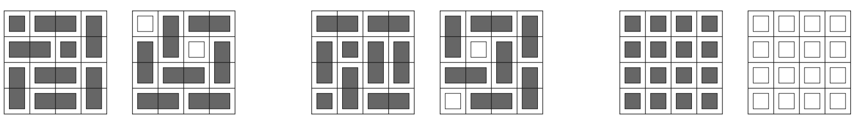

Figure 1.4: Three tilings $\mathbf{t}_1, \mathbf{t}_2, \mathbf{t}_{\mathrm{vert},2}$ of $[0,4]^2 \times [0,2]$. A straightforward verification shows that $\mathbf{t}_1 \not\approx \mathbf{t}_2$ but $\mathbf{t}_1 * \mathbf{t}_{\mathrm{vert},2} \approx \mathbf{t}_2 * \mathbf{t}_{\mathrm{vert},2}$, so that $\mathbf{t}_1 \sim \mathbf{t}_2$.

The notion of regular disk is presented in [22]. A nontrivial balanced quadriculated disk $\mathcal{D}$ is *regular* if whenever two tilings $\mathbf{t}_1$ and $\mathbf{t}_2$ of $\mathcal{D} \times [0, N]$ have the same twist then $\mathbf{t}_1$ and $\mathbf{t}_2$ can be connected by a sequence of flips once extra vertical space is added to the cylinder; equivalently, if $\mathrm{Tw}(\mathbf{t}_1) = \mathrm{Tw}(\mathbf{t}_2)$ then $\mathbf{t}_1 \sim \mathbf{t}_2$. We say that a disk is *irregular* if it is not regular. Saldanha [22] proved that the rectangle $\mathcal{D} = [0, L] \times [0, M]$ with LM even is regular if and only if $\min\{L, M\} \geq 3$; and it was conjectured that "plump" disks are regular.

For a regular disk $\mathcal{D}$, a natural question arises about the amount of additional vertical space required to ensure that any two tilings of a cylinder $\mathcal{R}_N$ with the same twist are equivalent under flips. In this context, Theorem 2 of [22] shows that there exists a constant $M_{\mathcal{D}} \in 2\mathbb{N}$ (not depending on N) such that any two tilings with the same twist become connected by flips when concatenated with the vertical tiling of height $M_{\mathcal{D}}$. However, even for small regions such as the 4×4 square, no estimates for $M_{\mathcal{D}}$ are known.

We dedicate a considerable part of this thesis to investigate the regularity of quadriculated disks. To this end, we study the *domino group* $G_{\mathcal{D}}$ of a disk $\mathcal{D}$. As a set, $G_{\mathcal{D}}$ is defined as the quotient

$$G_{\mathcal{D}} = \Big(\bigcup_{N \in \mathbb{N}} \mathcal{T}(\mathcal{R}_N) \Big) / \sim .$$

For simplicity, we abuse notation and represent elements of $G_{\mathcal{D}}$ by tilings, rather than their equivalence classes. The group operation on $G_{\mathcal{D}}$ is given by the concatenation. The identity element is the vertical tiling and the inverse of a tiling is obtained by taking its reflection on the xy plane. The well-definedness of concatenation under $\sim$ and the equivalence between a vertical tiling and a tiling concatenated with its inverse are detailed in Section 2.1. In Section 2.2, we present a useful alternative description of the domino group as the fundamental group of a CW-complex.

We frequently work with the *even domino group* $G^+_{\mathcal{D}}$, the normal subgroup of index two of $G_{\mathcal{D}}$ whose elements correspond to tilings of cylinders of even height. In general, $G^+_{\mathcal{D}}$ contains most of the relevant information for our discussion. Notably, the twist defines a homomorphism from $G_{\mathcal{D}}$ to the integers $\mathbb{Z}$, which maps $G^+_{\mathcal{D}}$ onto $\mathbb{Z}$ for nontrivial disks, implying that $G_{\mathcal{D}}$ is infinite; see Section 2.3. It turns out that a disk $\mathcal{D}$ is regular if and only if the restriction of this homomorphism to $G^+_{\mathcal{D}}$ is an isomorphism. In such cases, the domino group is a direct product of two groups: $G_{\mathcal{D}} = \mathbb{Z} \oplus \mathbb{Z}/(2)$.

We distinguish irregular disks by the behavior of their even domino groups. A disk $\mathcal{D}$ is called *strongly irregular* if there exists an epimorphism (i.e., a surjective homomorphism) from the even domino group $G^+_{\mathcal{D}}$ to F_2, the free group of rank two. The structure of $G^+_{\mathcal{D}}$ provides information about the space of tilings $\mathcal{T}(\mathcal{R}_N)$ for large values of N. In the regular case, where $G^+_{\mathcal{D}} = \mathbb{Z}$, it follows from [21] that the size of the largest connected component under flips is $\Theta(N^{-\frac{1}{2}}|\mathcal{T}(\mathcal{R}_N)|)$. We adopt a different but similar approach to prove that if $\mathcal{D}$ is strongly irregular then, for large N, the connected components consist of exponentially small fractions of $\mathcal{T}(\mathcal{R}_N)$. In probabilistic terms, this result is equivalent to Theorem 1.1.

Theorem 1.1. *Consider a nontrivial balanced quadriculated disk $\mathcal{D}$. If $\mathcal{D}$ is strongly irregular then there exists a constant $c \in (0,1)$ such that the following holds. Let $\mathbf{T}_1$ and $\mathbf{T}_2$ be two independent random tilings of $\mathcal{D} \times [0,N]$ then $\mathbb{P}(\mathbf{T}_1 \approx \mathbf{T}_2) = o(c^N)$.*

Remark 1.2. It follows from Theorem 12 of [21] that, for any nontrivial balanced disk $\mathcal{D}$, the probability $\mathbb{P}(\mathrm{Tw}(\mathbf{T}_1) = \mathrm{Tw}(\mathbf{T}_2))$ is asymptotically bounded below by N^{-1}. Thus, by Theorem 1.1, if $\mathcal{D}$ is strongly irregular, then $\mathbb{P}(\mathbf{T}_1 \approx \mathbf{T}_2 \mid \mathrm{Tw}(\mathbf{T}_1) = \mathrm{Tw}(\mathbf{T}_2))$ decreases exponentially with N. $\diamond$

The complete computation of the even domino group of a disk is not necessary to establish its strong irregularity; this appears to be a significantly more difficult task. From [22], we know that thin rectangles $\mathcal{D}_L = [0,L] \times [0,2]$ with $L \geq 3$ are strongly irregular. Inspired by the ideas presented in [19], we proceed to compute $G^+_{\mathcal{D}_L}$. Let $S_L = \{a_i \colon i \in \mathbb{Z}_{\neq 0} \text{ and } |i| \leq \lfloor \frac{L-1}{2} \rfloor\}$ be a set of symbols and let $R_L = \{(m,n) \in \mathbb{Z}^2 \colon \max\{|m|,|n|,|m-n|\} < \lfloor \frac{L}{2} \rfloor\}$. Now, consider the group described in terms of generators and relations

$$G^+_L = \langle S_L \mid [a_m, a_n] = 1 \text{ for } (m,n) \in R_L \rangle, \tag{1.1}$$

where $[a_m, a_n] = a_m a_n a_m^{-1} a_n^{-1}$ is the commutator of a_m and a_n. Therefore, in other words, G^+_L is the quotient of the free group on S_L by the normal subgroup generated by $[a_m, a_n]$ with $(m,n) \in R_L$.

Theorem 1.3. *Let $L \geq 3$ and consider the disk $\mathcal{D}_L = [0,L] \times [0,2]$. Then, the even domino group $G^+_{\mathcal{D}_L}$ is isomorphic to G^+_L.*

In most cases, we demonstrate the strong irregularity of a quadriculated disk $\mathcal{D}$ by explicitly constructing a surjective homomorphism from $G^+_{\mathcal{D}}$ to the free group F_2. This construction is based on the existence of floor configurations composed of dominoes arranged in a staggered configuration, as the fifth floor of the tiling exhibited in Figure 1.2. Although obtaining such disks is not too hard, their description can be somewhat intricate. For instance, the disks shown in Figures 1.5 and 1.6 are strongly irregular by Theorems 1.4 and 1.5, respectively. Additional constructions of strongly irregular disks are discussed in Section 5.2.

Theorem 1.4. *Let $\mathcal{D}$ be a balanced quadriculated disk $\mathcal{D}$. Suppose that $\mathcal{D}$ contains a unit square s such that $\mathcal{D} \smallsetminus s$ has at least three connected components. If the largest component of $\mathcal{D} \smallsetminus s$ has size at most $|\mathcal{D}| - 4$ then $\mathcal{D}$ is strongly irregular.*

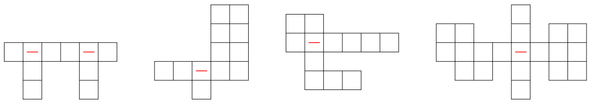

Figure 1.5: Examples of strongly irregular disks; unit squares s as in Theorem 1.4 are marked by a red line segment.

Theorem 1.5. *Let $\mathcal{D}$ be a balanced disk $\mathcal{D}$ containing a domino d such that $\mathcal{D} \smallsetminus d$ is not connected. Suppose there exists a 2×2 square in $\mathcal{D}$ containing d. If every connected component of $\mathcal{D} \smallsetminus d$ that intersects a 2×2 square in $\mathcal{D}$ containing d has size at most $\frac{|\mathcal{D}|-2}{2}$ then $\mathcal{D}$ is strongly irregular.*

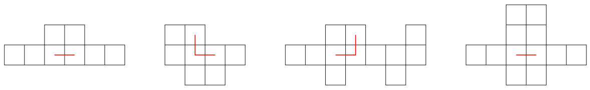

Figure 1.6: Examples of strongly irregular disks; dominoes d as in Theorem 1.5 are marked by a red line segment.

Disks that are irregular but not strongly irregular seem to be rare. Indeed, the only family of disks for which we demonstrate this phenomenon is as in Figure 1.7, whose details we present in Section 5.1. We believe that these are essentially the only examples of irregular but not strongly irregular disks. Notice that, in contrast with Theorem 1.4, these disks can be disconnected into three connected components by removing a unit square, with the largest component having size $|\mathcal{D}| - 3$.

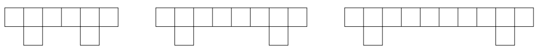

Figure 1.7: Examples of irregular disks that are not strongly irregular, for these disks the even domino group is isomorphic to $\mathbb{Z}^2$.

In addition to identifying irregular disks, we demonstrate that a substantial class of disks is regular. As a consequence, the disks depicted in Figures 1.8 and 1.9 are regular. Two properties, both with graph-theoretical interpretations, determine the regularity of a disk.

There exists a natural identification between a disk $\mathcal{D}$ and a bipartite graph $\mathcal{G}(\mathcal{D})$. The vertices of $\mathcal{G}(\mathcal{D})$ correspond to the unit squares in $\mathcal{D}$, and two vertices are connected by an edge if and only if their corresponding unit squares are adjacent. We refer to the properties of $\mathcal{G}(\mathcal{D})$ as properties of $\mathcal{D}$. In particular, $\mathcal{D}$ is called *hamiltonian* if $\mathcal{G}(\mathcal{D})$ has a hamiltonian cycle.

We also examine the presence of bottlenecks in $\mathcal{D}$, which are related to vertex cuts of size two of $\mathcal{G}(\mathcal{D})$. A bottleneck is defined by a domino $d \subset \mathcal{D}$ that *disconnects* $\mathcal{D}$, meaning that $\mathcal{D} \smallsetminus d$ is not connected. Notice that all examples of irregular disks presented in this thesis contain bottlenecks. In fact, we conjecture that disks free of bottlenecks are regular.

Our first result on regular disks, which can be viewed as a particular case of the second, establishes the regularity of bottleneck-free hamiltonian disks. The second result shows the regularity of a hamiltonian disk obtained by introducing narrow and small bottlenecks into an initially bottleneck-free disk.

Theorem 1.6. *Let $\mathcal{D}$ be a nontrivial hamiltonian quadriculated disk. Suppose that there exists no domino $d \subset \mathcal{D}$ such that $\mathcal{D} \smallsetminus d$ is not connected. Then, $\mathcal{D}$ is regular.*

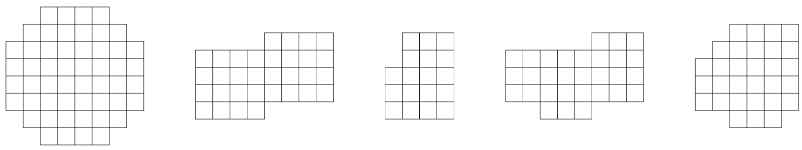

Figure 1.8: Examples of disks whose regularity follows from Theorem 1.6.

Theorem 1.7. *Let $\mathcal{D}_0$ be a disk satisfying the hypothesis of Theorem 1.6. Consider pairwise disjoint disks $\mathcal{D}_1, \ldots, \mathcal{D}_k$ such that $|\mathcal{D}_i| < |\mathcal{D}_0| - 2$ and $\mathcal{D}_i \cap \mathcal{D}_0$ is a line segment of length two. If $\mathcal{D} = \bigcup_{i=0}^{k} \mathcal{D}_i$ is a hamiltonian disk then $\mathcal{D}$ is regular.*

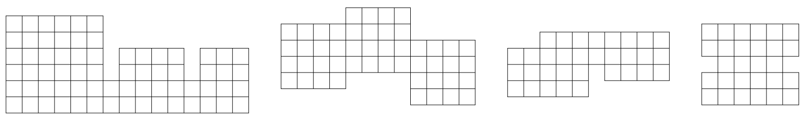

Figure 1.9: Examples of disks whose regularity follows from Theorem 1.7.

Naturally, Theorems 1.6 and 1.7 motivate the question of whether a bottleneck-free disk is hamiltonian, which is equivalent to determining whether a solid grid graph with no vertex cut of size two formed by adjacent vertices has a hamiltonian cycle. Zamfirescu and Zamfirescu [26] showed that certain grid graphs with width greater than two are hamiltonian. Conversely, Keshavarz-Kohjerdi and Bagheri [11] established conditions that a hamiltonian rectangular truncated grid graph must satisfy. As a consequence, the first two disks in Figure 1.10 are not hamiltonian. On the other hand, it is easy to obtain examples of disks with small bottlenecks that fail to be hamiltonian, as the last two disks in Figure 1.10. Although our theorems do not apply directly, the regularity of these four disks can be easily established by combining our results with an additional analysis, as each disk becomes hamiltonian after the removal of two specific unit squares. On a positive note, in light of Theorem 1.5, the inequality in Theorem 1.7 regarding the size of the pairwise disjoint disks is tight.

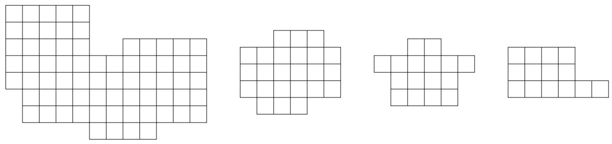

Figure 1.10: Four regular disks.

This thesis is based on the preprints [15] and [17].

2
Definitions

This chapter provides the necessary background to establish our results. The content follows [22], the definitions and results are included to ensure the text is self-contained. To avoid repetition, proofs are omitted.

The first section focuses on constructing a particular family of generators of the even domino group of *path-hamiltonian* disks, i.e., disks whose associated bipartite graph has a hamiltonian path. The second section presents an alternative formulation of the domino group of a disk, which is particularly useful for demonstrating the irregularity of disks. The third section is dedicated to the definition of the twist of a tiling.

2.1
Plugs, corks and generators

Throughout this text we routinely abuse notation and neglect boundaries when discussing quadriculated regions. Given two regions $\mathcal{R}$ and $\widetilde{\mathcal{R}}$, we write $\mathcal{R} \smallsetminus \widetilde{\mathcal{R}}$ for the quadriculated region formed by the closed unit squares that are in $\mathcal{R}$ but not in $\widetilde{\mathcal{R}}$. Similarly, we say that $\mathcal{R}$ and $\widetilde{\mathcal{R}}$ are disjoint if they do not share any unit square. In that sense, two unit squares that have only one or two vertices in common are said to be disjoint. Henceforth, unless stated otherwise, we assume that all quadriculated disks are nontrivial and balanced.

Let $\mathcal{D}$ be a quadriculated disk. A *plug* $p \subset \mathcal{D}$ is a balanced subregion of $\mathcal{D}$, that is, a union of an equal number of white and black closed unit squares contained in $\mathcal{D}$; examples of plugs are exhibited in Figure 2.1. We distinguish the *empty plug* $\mathbf{p}_\circ = \varnothing$ and the *full plug* $\mathbf{p}_\bullet = \mathcal{D}$. The complement $p^{-1} = \mathcal{D} \smallsetminus p$ of a plug p is also a plug. We denote by $|p|$ the number of unit squares in p and by $\mathcal{P}$ the set of plugs in $\mathcal{D}$.

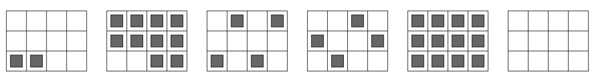

Figure 2.1: Six plugs of $\mathcal{D} = [0,4] \times [0,3]$. The first plug is a domino and its complement is the second plug, the third and fourth plugs are disjoint, the fifth plug is the full plug and the last plug is the empty plug.

Sometimes, it is useful to consider regions more general than cylinders. Let $p_1, p_2 \in \mathcal{P}$ be two plugs and consider two nonnegative integers N_1 and N_2 such that $N_2 > N_1 + 2$. The *cork* $\mathcal{R}_{N_1,N_2;p_1,p_2}$ is defined as:

$$\mathcal{R}_{N_1,N_2;p_1,p_2} = (\mathcal{D} \times [N_1+1, N_2-1]) \cup (p_1^{-1} \times [N_1, N_1+1]) \cup (p_2^{-1} \times [N_2-1, N_2]).$$

In other words, $\mathcal{R}_{N_1,N_2;p_1,p_2}$ is obtained from $\mathcal{D}\times[N_1,N_2]$ by removing the plug p_1 from the (N_1+1)-th floor and the plug p_2 from the N_2-th floor. For instance, $\mathcal{R}_{0,N;\mathbf{p}_\circ,\mathbf{p}_\circ}=\mathcal{R}_N$. The set of tilings of $\mathcal{R}_{N_1,N_2;p_1,p_2}$ is denoted by $\mathcal{T}(\mathcal{R}_{N_1,N_2;p_1,p_2})$.

A *floor* is a triple $f=(p_1,f^*,p_2)$, where p_1 and p_2 are two disjoint plugs and f^* is a set of planar dominoes that defines a tiling of $\mathcal{D}\smallsetminus(p_1\cup p_2)$. We refer to f^* as the *reduced floor*, and we call f a *vertical floor* if $f^*=\varnothing$. Notice that the inverse $f^{-1}=(p_2,f^*,p_1)$ of a floor f is also a floor.

We have an identification between tilings of corks (in particular, cylinders) and sequences of floors. Indeed, as in Figure 1.2, tilings are essentially drawn by exhibiting their corresponding sequences of floors. More specifically, consider a tiling $\mathbf{t}$ of $\mathcal{R}_{0,N;p_1,p_2}$. The behavior of $\mathbf{t}$ at $\mathcal{D}\times[K-1,K]$ is determined by a floor $f_K=(p_{1,K},f_K^*,p_{2,K})$. The plug $p_{i,K}$ consists of the unit squares $[a,a+1]\times[b,b+1]$ such that $[a,a+1]\times[b,b+1]\times[K-3+i,K-1+i]$ is a vertical domino in $\mathbf{t}$, while f_K^* corresponds to the horizontal dominoes of $\mathbf{t}$ contained in $\mathcal{D}\times[K-1,K]$. Thus, $p_{1,K}$ and $p_{2,K}$ are disjoint and $p_{1,K}=p_{2,K-1}$; with the conventions $p_{1,1}=p_1$ and $p_{2,N}=p_2$. Therefore, $\mathbf{t}$ is completely described by a concatenation of floors: $\mathbf{t}=f_1*f_2*\ldots*f_N$. Similarly, a tiling can be described as a concatenation of tilings of corks and floors. Figure 2.2 illustrates an example of this construction.

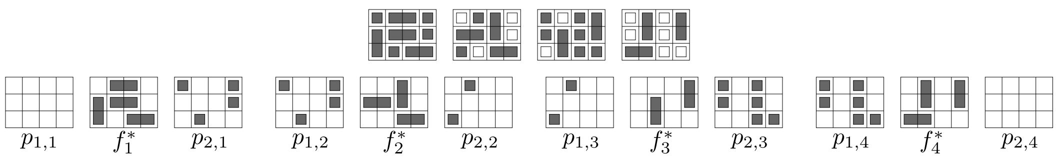

Figure 2.2: A tiling of $\mathcal{D}\times[0,4]$ with $\mathcal{D}=[0,4]\times[0,3]$ and its description by the four floors $f_K=(p_{1,K},f_K^*,p_{2,K})$. Notice that $p_{1,1}=p_{2,4}=\mathbf{p}_\circ$.

An important fact is that pairs of vertical floors can be moved through flips. For instance, consider a tiling $\mathbf{t}=\mathbf{t}_1*\mathbf{t}_2$ with $\mathbf{t}_1\in\mathcal{T}(\mathcal{R}_{0,N_1;\mathbf{p}_\circ,p_1})$ and $\mathbf{t}_2\in\mathcal{T}(\mathcal{R}_{0,N_2;p_1,\mathbf{p}_\circ})$. It turns out that $\mathbf{t}*\mathbf{t}_{\text{vert},2}\approx\mathbf{t}_1*\mathbf{t}_{\text{vert},p_1}*\mathbf{t}_2\approx\mathbf{t}_{\text{vert},2}*\mathbf{t}$, where $\mathbf{t}_{\text{vert},p_1}\in\mathcal{T}(\mathcal{R}_{0,2;p_1,p_1})$ is the tiling formed only by vertical dominoes (see Lemma 5.3 of [22]). Therefore, the relation $\sim$ allows the addition of an arbitrary even number of vertical floors between any two floors of a tiling. In particular, concatenation is well-defined under $\sim$.

The inverse of a tiling $\mathbf{t}$ of $\mathcal{R}_{N_1,N_2;p_1,p_2}$ is defined as the tiling $\mathbf{t}^{-1}$ of $\mathcal{R}_{N_1,N_2;p_2,p_1}$ obtained by reflecting $\mathbf{t}$ on the xy plane. In the language of floors, if $\mathbf{t}=f_1*f_2*\ldots*f_N$ then $\mathbf{t}^{-1}=f_N^{-1}*f_{N-1}^{-1}*\ldots*f_1^{-1}$. We have $\mathbf{t}*\mathbf{t}^{-1}\sim\mathbf{t}_{\text{vert},p_1}$ (see Lemma 4.2 of [22]).

A *path of length* k is a sequence $\gamma=(s_1,s_2,\ldots,s_k)$ of distinct unit squares in $\mathcal{D}$ such that s_i and s_{i+1} are adjacent for all i. We say that γ is a *cycle* if the initial and final squares s_1 and s_k are also adjacent. Therefore, a disk $\mathcal{D}$ is path-hamiltonian (resp. hamiltonian) if and only if it has a path (resp. cycle) of length $|\mathcal{D}|$. Figure 2.3 shows examples of hamiltonian cycles and paths, their orientation and initial square are indicated by an arrow.

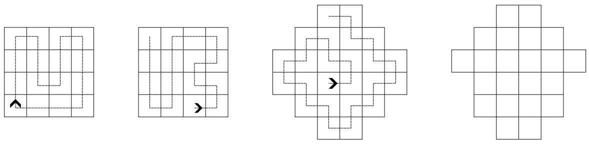

Figure 2.3: The first and the second example show a hamiltonian cycle and a hamiltonian path in $[0,4]^2$. The third disk is path-hamiltonian but not hamiltonian. The fourth disk is neither path-hamiltonian nor hamiltonian.

From now on, until the end of this section, consider a disk $\mathcal{D}$ with a fixed hamiltonian path $\gamma = (s_1, s_2, \ldots, s_{|\mathcal{D}|})$. We proceed towards the construction of a family of tilings that generates the even domino group $G^+_{\mathcal{D}}$. Clearly, the following arguments apply similarly to hamiltonian cycles, as we can transform any cycle into a path by separating its initial and final squares.

We first need the notion of whether a domino respects γ. A domino $d \subset \mathcal{D}$ *respects* γ if it is equal the union of s_i and s_{i+1} for some i. A three-dimensional domino $d \subset \mathcal{R}_N$ *respects* γ if its projection on $\mathcal{D}$ is either a unit square or a planar domino that respects γ. In view of Fact 2.1, it will be important to consider the set $\mathcal{D}_\gamma$ composed by the dominoes in $\mathcal{D}$ that do not respect γ.

Fact 2.1 (Lemma 8.1 of [22])**.** *Let $\mathcal{D}$ be a disk with a hamiltonian path γ. If $\mathbf{t} \in \mathcal{T}(\mathcal{R}_{0,2N;p,p})$ is a tiling whose dominoes respect γ then $\mathbf{t} \sim \mathbf{t}_{vert,p}$.*

For each plug $p \in \mathcal{P}$, we construct a tiling $\mathbf{t}_p \in \mathcal{T}(\mathcal{R}_{0,|p|;p,\mathbf{p}_\circ})$ whose dominoes respect γ; by convention, $\mathbf{t}_{\mathbf{p}_\circ} = \varnothing$. To this end, it suffices to describe the horizontal dominoes contained in each floor of $\mathbf{t}_p$. We proceed by induction on $|p|$. Consider two unit squares of opposite colors $s_i, s_j \subset p$ with $i < j$ and $j-i$ minimal. If $j = i+1$, the first floor (of $\mathbf{t}_p$) contains no horizontal dominoes. Otherwise, the horizontal dominoes of the first floor are obtained by placing dominoes along the path $(s_{i+1}, s_{i+2}, \ldots, s_{j-1})$, more precisely, $s_{i+1} \cup s_{i+2}$, $s_{i+3} \cup s_{i+4}, \ldots,$ $s_{j-2} \cup s_{j-1}$. Similarly, the horizontal dominoes of the second floor are obtained by placing dominoes along the path $(s_i, s_{i+1}, \ldots, s_j)$. The concatenation of these two floors with $\mathbf{t}_{p \smallsetminus (s_i \cup s_j)}$ (that we already constructed by induction) defines $\mathbf{t}_p$; for an example, see Figure 2.4. Notice that different choices of unit squares at minimal distance yield distinct tilings, which are connected through flips by Fact 2.1.

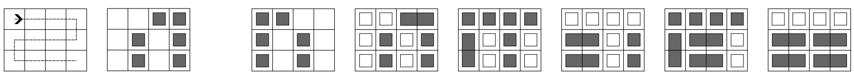

Figure 2.4: A disk with a hamiltonian path, a plug p and the tiling $\mathbf{t}_p$.

Remark 2.2. We can also obtain a tiling of $\mathcal{R}_{0,|p|;p,\mathbf{p}_\circ}$ even when $\mathcal{D}$ is not path-hamiltonian. By considering a spanning tree of $\mathcal{D}$, the same procedure of using unit squares at minimal distances produces a tiling $\mathbf{t}_p$. However, Fact 2.1 no longer applies in this scenario, and distinct choices of unit squares at minimal distance may result in tilings that are not equivalent under $\sim$. ◇

Consider a floor $f = (p_1, f^*, p_2)$. Let $f_{\text{vert}} = (p_2, \varnothing, p_2^{-1})$ be a vertical floor. Then, set $\mathbf{t}_f = \mathbf{t}_{p_1}^{-1} * f * f_{\text{vert}} * \mathbf{t}_{p_2^{-1}} \in \mathcal{T}(\mathcal{R}_N)$ where $N = |p_1| + |p_2^{-1}| + 2$. Notice that dominoes in $\mathbf{t}_f$ that do not respect γ must be in the floor f.

Fact 2.3 (Lemma 8.2 of [22][1])**.** *Let $\mathcal{D}$ be a disk with a hamiltonian path γ. Consider N even and a tiling $\mathbf{t} \in \mathcal{T}(\mathcal{R}_N)$ with floors $f_1, f_2, \ldots, f_N$, so that $\mathbf{t} = f_1 * f_2 * \ldots * f_N$. Then,*

$$\mathbf{t} \sim \mathbf{t}_{f_1} * \mathbf{t}_{f_2^{-1}}^{-1} * \ldots * \mathbf{t}_{f_i^{(-1)^{(i+1)}}}^{(-1)^{(i+1)}} * \ldots * \mathbf{t}_{f_N^{-1}}^{-1}.$$

We now consider a particular case of the construction above. A plug and a domino $d \subset \mathcal{D}$ are *compatible* if they are disjoint, the set of plugs compatible with d is denoted by $\mathcal{P}_d$. For a domino $d \subset \mathcal{D}$ with a compatible plug $p \in \mathcal{P}_d$, let $f = (p, d, (p \cup d)^{-1})$ be a floor and set $\mathbf{t}_{d,p;\gamma} = \mathbf{t}_f$; when the context is clear we write $\mathbf{t}_{d,p}$ instead of $\mathbf{t}_{d,p;\gamma}$. Notice that if $d \notin \mathcal{D}_\gamma$ then Fact 2.1 implies that $\mathbf{t}_{d,p} \sim \mathbf{t}_{\text{vert}}$. On the other hand, if $d \in \mathcal{D}_\gamma$ then $d \times [|p|, |p| + 1]$ is the only domino in $\mathbf{t}_{d,p}$ that does not respect γ. For instance, see Figure 2.5.

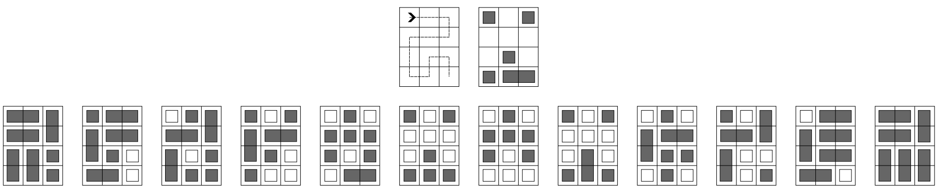

Figure 2.5: The first row shows the disk $\mathcal{D} = [0, 3] \times [0, 4]$ with a hamiltonian path γ, and a domino d with a compatible plug p. The second row shows $\mathbf{t}_{d,p;\gamma} = \mathbf{t}_p^{-1} * f * f_{\text{vert}} * \mathbf{t}_{p \cup d}$.

Fact 2.4 (Lemma 8.3 of [22])**.** *Let $\mathcal{D}$ be a disk with a hamiltonian path γ. Consider a floor $f = (p, f^*, \tilde{p})$. Suppose that $f^* = \{d_1, d_2, \ldots, d_k\}$. Let $p_1 = p$ and $p_{i+1} = p_i \cup d_i$. Then,*

$$\mathbf{t}_f \sim \mathbf{t}_{d_1,p_1} * \ldots * \mathbf{t}_{d_i,p_i} * \ldots * \mathbf{t}_{d_k,p_k}.$$

Notice that Facts 2.3 and 2.4 imply that the even domino group $G_{\mathcal{D}}^+$ is generated by the set of tilings of the form $\mathbf{t}_{d,p}$. It is possible to reduce this family

[1]There is a typo in the original result, and the -1 superscripts on the floors of even parity are missing.

of generators through the notion of flux between a domino and a plug, which we now define. In order to define flux, it is important to distinguish whether a unit square is black or white. To facilitate this distinction, we utilize the path γ. For a unit square s_i, define $\mathrm{color}(s_i) = (-1)^i$. Then, s_i is identified as white if $\mathrm{color}(s_i) = +1$ and as black if $\mathrm{color}(s_i) = -1$.

Consider a domino $d \in \mathcal{D}_\gamma$, so that $d = s_k \cup s_l$ with $l - k > 1$. The domino d decomposes the region $\mathcal{D} \setminus d$ into three subregions:

$$\mathcal{D}_{d,-1} = \bigcup_{i=1}^{k-1} s_i, \qquad \mathcal{D}_{d,0} = \bigcup_{i=k+1}^{l-1} s_i, \qquad \mathcal{D}_{d,+1} = \bigcup_{i=l+1}^{|\mathcal{D}|} s_i.$$

Clearly, each region $\mathcal{D}_{d,j}$ comes with a hamiltonian path $\gamma_{d,j}$. The regions $\mathcal{D}_{d,-1}$ and $\mathcal{D}_{d,+1}$ are not necessarily balanced and nonempty. However, $\mathcal{D}_{d,0}$ is always balanced and nonempty, as $l - k > 1$ and $(s_k, s_{k+1}, \ldots, s_l)$ is a cycle. The union of $\mathcal{D}_{d,-1}$ and $\mathcal{D}_{d,+1}$ is denoted by $\mathcal{D}_{d,\pm 1}$.

Consider a plug $p \in \mathcal{P}_d$ compatible with d, we define a triple of integers $\mathrm{flux}(d,p) = (\mathrm{flux}_{-1}(d,p), \mathrm{flux}_0(d,p), \mathrm{flux}_{+1}(d,p)) \in \mathbb{Z}^3$. The coordinate $\mathrm{flux}_j(d,p)$ is computed by summing $\mathrm{color}(s_i) = (-1)^i$ over the unit squares s_i contained in $p \cap \mathcal{D}_{d,j}$. Notice that $\mathrm{flux}_{-1}(d,p) + \mathrm{flux}_0(d,p) + \mathrm{flux}_{+1}(d,p) = 0$, since p is a balanced subregion of $\mathcal{D}$.

Fact 2.5 (Lemma 8.4 of [22]). *Let $\mathcal{D}$ be a disk with a hamiltonian path γ. Consider a domino $d \in \mathcal{D}_\gamma$ and two plugs $p_1, p_2 \in \mathcal{P}_d$. If $\mathrm{flux}(d,p_1) = \mathrm{flux}(d,p_2)$ then $\mathbf{t}_{d,p_1} \sim \mathbf{t}_{d,p_2}$*

Consequently, we obtain a family of generators of $G^+_\mathcal{D}$ as follows.

Fact 2.6 (Corollary 8.6 of [22]). *Consider a disk $\mathcal{D}$ with a hamiltonian path γ. For each domino $d \in \mathcal{D}_\gamma$, let Φ_d be the set of the possible triples $\mathrm{flux}(d,\cdot)$. For each $\phi \in \Phi_d$, consider a plug $p_{d,\phi} \in \mathcal{P}_d$ such that $\mathrm{flux}(d, p_{d,\phi}) = \phi$. The even domino group $G^+_\mathcal{D}$ is generated by the family of tilings $(\mathbf{t}_{d,p_{d,\phi}})$.*

2.2 The domino complex

Given a quadriculated disk $\mathcal{D}$, we construct a 2-dimensional CW-complex $\mathcal{C}_\mathcal{D}$ called *domino complex*. The domino group $G_\mathcal{D}$ will correspond to the the fundamental group of $\mathcal{C}_\mathcal{D}$. The key idea is to associate each tiling of $\mathcal{R}_N$ with an oriented closed path of length N in the 1-skeleton of $\mathcal{C}_\mathcal{D}$. To this end, we convert the description of a tiling as a concatenation of floors into an oriented path in $\mathcal{C}_\mathcal{D}$ by assigning an oriented edge to each possible floor configuration. The 2-cells are then attached to attend flips.

The 0-skeleton, the set of vertices of $\mathcal{C}_\mathcal{D}$, is the set of plugs $\mathcal{P}$. The edges of $\mathcal{C}_\mathcal{D}$ represent two-dimensional domino tilings of subregions of $\mathcal{D}$. More precisely, attach an edge between two disjoint plugs p_1 and p_2 for each tiling of $\mathcal{D} \smallsetminus (p_1 \cup p_2)$. In particular, plugs that are not disjoint do not share any edge. For the special case $p_1 = p_2 = \mathbf{p}_\circ$ (the empty plug), there is a loop based at $\mathbf{p}_\circ$ for each tiling of $\mathcal{D}$; there are no other loops in $\mathcal{C}_\mathcal{D}$. This construction defines the 1-skeleton of $\mathcal{C}_\mathcal{D}$.

We now attach the 2-cells. First, attach a disk to each loop by wrapping its boundary twice around the loop, so that the result is a projective plane. In other words, each loop f is homotopically equivalent to a circle, and we attach a disk via the map $f * f$. For instance, see Figure 2.6.

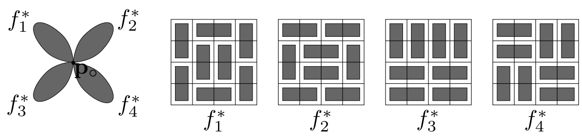

Figure 2.6: Four loops in the complex $\mathcal{C}_\mathcal{D}$ for $\mathcal{D} = [0,4]^2$, the four petals are four projective planes.

The other 2-cells correspond to horizontal and vertical flips, and are attached injectively to certain bigons and quadrilaterals. Notice that a bigon consists of two distinct disjoint plugs p_1 and p_2 connected by two edges representing distinct tilings of $\mathcal{D} \smallsetminus (p_1 \cup p_2)$. We attach a disk to each bigon whose edges correspond to tilings which differ by a single flip, as in Figure 2.7.

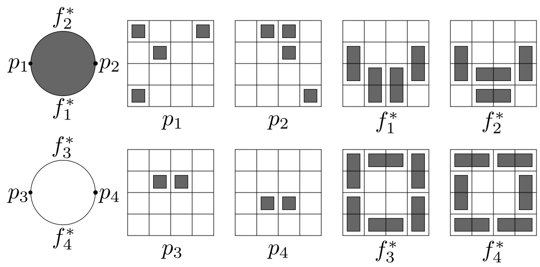

Figure 2.7: Two bigons in the complex of $\mathcal{D} = [0,4]^2$. In the first row we attach a disk to the bigon. The two tilings in the second row do not differ by a single flip. Therefore, we do not attach a disk to the bigon in the second row.

We attach a 2-cell to quadrilaterals corresponding to a single vertical flip, each such quadrilateral is constructed as follows. Let p_1, p_2, p_3, p_4 be four plugs such that p_2 is disjoint from p_1 and p_4. Suppose that p_2 equals a union of p_3 and two adjacent unit squares, i.e. a domino $d \subset \mathcal{D}$. Let f_1^* be a tiling of $\mathcal{D} \smallsetminus (p_1 \cup p_2)$ and f_2^* be a tiling of $\mathcal{D} \smallsetminus (p_2 \cup p_4)$. Therefore, $f_3^* = f_1^* \cup d$ and $f_4^* = f_2^* \cup d$ are tilings of $\mathcal{D} \smallsetminus (p_1 \cup p_3)$ and $\mathcal{D} \smallsetminus (p_3 \cup p_4)$, respectively. Notice that p_1, p_2, p_3, p_4 and $f_1^*, f_2^*, f_3^*, f_4^*$ thus define a quadrilateral in the 1-skeleton of $\mathcal{C}_\mathcal{D}$. Then, attach a 2-cell to this quadrilateral, as in Figure 2.8.

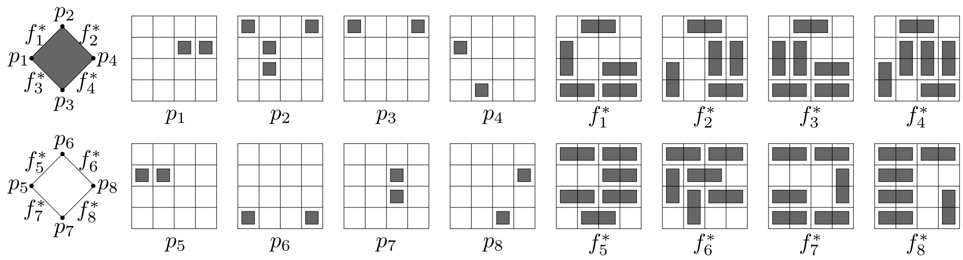

Figure 2.8: Two quadrilaterals in the complex of $\mathcal{D} = [0, 4]^2$. In the first row we attach a 2-cell to the quadrilateral. The second row shows an example of a quadrilateral where we do not attach a 2-cell.

This finishes the construction of the complex $\mathcal{C}_\mathcal{D}$. In most cases, it is impractical to draw the complex $\mathcal{C}_\mathcal{D}$. For instance, if $\mathcal{D} = [0, 4]^2$ then $\mathcal{C}_\mathcal{D}$ has 12870 vertices and 36 loops. The calculation of the exact number of 1-cells and 2-cells requires a long computation.

In the complex $\mathcal{C}_\mathcal{D}$, we specify an orientation each time we move along an edge. Consider two distinct disjoint plugs p_1 and p_2 and let f_1^* be a tiling of $\mathcal{D} \smallsetminus (p_1 \cup p_2)$, so that f_1^* is an edge of $\mathcal{C}_\mathcal{D}$. We then denote the two possible orientations of f_1^* through the language of floors , i.e. , by $f = (p_1, f_1^*, p_2)$ and $f^{-1} = (p_2, f_1^*, p_1)$. Notice that, since projective planes are attached to loops, the two possible orientations of a loop $f = (\mathbf{p}_\circ, f^*, \mathbf{p}_\circ)$ are homotopic.

The complex $\mathcal{C}_\mathcal{D}$ is related to tilings of cylinders of base $\mathcal{D}$. Indeed, recall from Section 2.1 that a tiling $\mathbf{t}$ of $\mathcal{D} \times [0, N]$ can be represented as sequence of floors $\mathbf{t} = f_1 * f_2 * \ldots * f_N$. By the previous paragraph, the tiling $\mathbf{t}$ is then described in $\mathcal{C}_\mathcal{D}$ by a closed oriented path of length N based at $\mathbf{p}_\circ$.

Under this identification of tilings and paths, concatenation of paths in $\mathcal{C}_\mathcal{D}$ corresponds to concatenation of tilings. In that sense, flips correspond to homotopies between paths. Then, two tilings are equivalent under $\sim$ if and only if their corresponding paths in $\mathcal{C}_\mathcal{D}$ are homotopic (see Lemma 5.4 of [22]). We then have that $G_\mathcal{D} = \pi_1(\mathcal{C}_\mathcal{D}, \mathbf{p}_\circ)$.

The even domino group $G_\mathcal{D}^+$ is a normal subgroup of index two of $G_\mathcal{D}$. Then, $G_\mathcal{D}^+$ is the fundamental group of a double cover $\mathcal{C}_\mathcal{D}^+$ of $\mathcal{C}_\mathcal{D}$, i.e., $\pi_1(\mathcal{C}_\mathcal{D}^+) = G_\mathcal{D}^+$. The set of vertices of $\mathcal{C}_\mathcal{D}^+$ is the set $\mathcal{P} \times \mathbb{Z}/(2)$, which indicates the plug and the parity of its position. Moreover, if p_1 and p_2 are two disjoint plugs then each tiling f_1^* of $\mathcal{D} \smallsetminus (p_1 \cup p_2)$ corresponds to two edges in $\mathcal{C}_\mathcal{D}^+$. Indeed, for each $i \in \mathbb{Z}/(2)$, there is an edge $f_{1,i}^*$ between $(p_1, i+1)$ and (p_2, i). Therefore, $\mathbf{f}_i = ((p_1, i+1), f_{1,i}^*, (p_2, i))$ and $\mathbf{f}_i^{-1} = ((p_2, i), f_{1,i}^*, (p_1, i+1))$ define two orientations of $f_{1,i}^*$. We prefer to describe the orientation of an edge in $\mathcal{C}_\mathcal{D}^+$ by a pair formed by an oriented edge in $\mathcal{C}_\mathcal{D}$ and an element $i \in \mathbb{Z}/(2)$.

The oriented edge of $\mathcal{C}_{\mathcal{D}}$ indicates the initial and the final vertex, the element of $\mathbb{Z}/(2)$ indicates the parity of the final vertex. For instance, an oriented edge $\mathbf{f}_i = ((p_1, i+1), f^*_{1,i}, (p_2, i))$ in $\mathcal{C}^+_{\mathcal{D}}$ is described by the pair (f, i) where $f = (p_1, f^*_1, p_2)$ is an oriented edge in $\mathcal{C}_{\mathcal{D}}$. Therefore, oriented edges in $\mathcal{C}^+_{\mathcal{D}}$ are also called *floors with parity*. Notice that if $\mathbf{f}_i = (f, i)$ then $\mathbf{f}_i^{-1} = (f^{-1}, i+1)$.

2.3 Twist

In this section, we briefly recall the definition of the twist of a tiling. First, fix a black and white coloring of the unit cubes in $\mathbb{R}^3$ such that adjacent cubes have opposite colors. For example, identify a cube $[a, a+1] \times [b, b+1] \times [c, c+1]$, with $(a, b, c) \in \mathbb{Z}^3$, as white if $a+b+c$ is even and as black if $a+b+c$ is odd.

For a three-dimensional domino d, let $v(d) \in \{\pm e_1, \pm e_2, \pm e_3\} \subset \mathbb{R}^3$ denote the unit vector from the center of the white cube to the center of the black cube of d. Consider a direction $u \in \{\pm e_1, \pm e_2\}$ and define $\mathcal{S}^u(d)$ as the interior of the set $(\bigcup_{t \in [0,\infty)} d + tu) \setminus d$.

Given a tiling $\mathbf{t}$ of $\mathcal{D} \times [0, N]$ and two dominoes d_1 and d_2 of $\mathbf{t}$ let

$$\tau^u(d_1, d_2) = \begin{cases} \frac{1}{4}\det(v(d_2), v(d_1), u), & d_2 \cap \mathcal{S}^u(d_1) \neq \emptyset \\ 0, & \text{otherwise} \end{cases}$$

Notice that $\tau^u(d_1, d_2) = 0$ unless d_1 is a vertical domino and d_2 is a horizontal domino (or vice versa), with both contained in $\mathcal{D} \times [K, K+2]$ for some K.

The *twist* of $\mathbf{t}$ is defined as the sum:

$$\operatorname{Tw}(\mathbf{t}) = \sum_{d_1, d_2 \in \mathbf{t}} \tau^u(d_1, d_2)$$

From the definition, it is not difficult to see that the value of the twist is not affected by flips. Moreover, we have that $\operatorname{Tw}(\mathbf{t}^{-1}) = -\operatorname{Tw}(\mathbf{t})$ and $\operatorname{Tw}(\mathbf{t}_1 * \mathbf{t}_2) = \operatorname{Tw}(\mathbf{t}_1) + \operatorname{Tw}(\mathbf{t}_2)$ for any two tilings $\mathbf{t}_1 \in \mathcal{T}(\mathcal{R}_{N_1})$ and $\mathbf{t}_2 \in \mathcal{T}(\mathcal{R}_{N_2})$. A more subtle property is that the twist is always an integer and is independent of the choice of u (see [18]).

Therefore, the twist defines a homomorphism $\operatorname{Tw}\colon G_{\mathcal{D}} \to \mathbb{Z}$. In the case that $\mathcal{D}$ is a nontrivial balanced disk, the twist maps $G^+_{\mathcal{D}}$ onto $\mathbb{Z}$. Thus, the twist and its restriction to the even domino group are surjective homomorphisms.

Fact 2.7 (Lemma 6.2 of [22]). *Let $\mathcal{D}$ be a nontrivial balanced disk. There exist $N \in 2\mathbb{N}$ and $\mathbf{t} \in \mathcal{T}(\mathcal{R}_N)$ such that $\operatorname{Tw}(\mathbf{t}) = 1$. In particular, the restriction $\operatorname{Tw}\colon G^+_{\mathcal{D}} \to \mathbb{Z}$ is surjective.*

3
Flip connected components of strongly irregular disks

In this chapter, we prove Theorem 1.1. The strategy of the proof involves the following steps. We begin by establishing a general result on random tilings of cylinders. For a disk $\mathcal{D}$, we show that for any fixed family of tilings of $\mathcal{R}_{N_0}$, the probability that a random tiling of $\mathcal{R}_N$ contains few tilings from the fixed family decays exponentially as N goes to infinity. We then associate the probability that two (independent) random tilings of $\mathcal{R}_N$ are equivalent under flips with the probability of a random tiling, formed alternately by concatenations of tilings from the fixed family with others not in the family, equals the vertical tiling. Given a surjective homomorphism $\phi\colon G^+_{\mathcal{D}} \to F_2$, where F_2 is the free group generated by a and b with e as the identity, we consider a fixed family of tilings corresponding to the values a, a^{-1}, b, b^{-1}, e. By taking the image under ϕ, we then relate the probability that two random tilings are equivalent under flips to the probability that a lazy random walk on F_2, which takes a deterministic step after each random step, returns to the identity. Theorem 1.1 then follows from the fact that the later probability decays exponentially as the length of the walk increases; as we show in the subsequent section.

3.1
Permuted random walks

The main result of this section is Lemma 3.1 below. The first part of this result was recently independently proved (in greater generality) in [1], while the second part follows from a combination of the first part and the well known fact that the return probabilities of a random walk on F_2 decay exponentially (e.g., the Varopoulos-Carne bound).

Lemma 3.1. *Let $s \in (0, \frac{1}{8})$. Let $(X_t)_{t\geq 1}$ be a sequence of i.i.d. random variables in F_2 such that $\mathbb{P}(X_1 = a) = \mathbb{P}(X_1 = b) = \mathbb{P}(X_1 = a^{-1}) = \mathbb{P}(X_1 = b^{-1}) = s$ and $\mathbb{P}(X_1 = e) = 1 - 4s$. Consider a sequence $(y_t)_{t\geq 0}$ of elements in F_2. Then the following holds*

1. $\mathbb{P}(y_0X_1y_1 \dots X_ty_t = e) \leq \mathbb{P}(X_1 \dots X_t = e)$ *for all* $t \geq 0$
2. *There is* $\alpha \in (0, 1)$ *such that* $\mathbb{P}(y_0X_1y_1 \dots X_ty_t = e) \leq \alpha^t$ *for all* $t \geq 0$.

We first establish a few combinatorial lemmas about finite subsets of F_2. Henceforth, we speak of a subset in F_2 and its corresponding forest in the

Cayley graph of F_2 interchangeably. We order the words in F_2 in increasing order of length by stipulating that $a < b < a^{-1} < b^{-1}$ and then following the alphabetical order. For each $n \geq 1$, let v_{n-1} denote the n-th word in F_2. Then, for instance, the first twelve words are: $v_0 = e$, $v_1 = a$, $v_2 = b$, $v_3 = a^{-1}$, $v_4 = b^{-1}$, $v_5 = aa$, $v_6 = ab$, $v_7 = ab^{-1}$, $v_8 = ba$, $v_9 = bb$, $v_{10} = ba^{-1}$, $v_{11} = a^{-1}b$.

Fix a positive real number $s < \frac{1}{8}$. Consider a finite set $M \subset F_2$ and let $\mathbf{1}_M$ be the characteristic function of M. Define the weight function $w_M \colon F_2 \to \mathbb{R}$ by $w_M(v) = (1-4s)\mathbf{1}_M(v) + s(\mathbf{1}_M(va) + \mathbf{1}_M(vb) + \mathbf{1}_M(va^{-1}) + \mathbf{1}_M(vb^{-1}))$. Notice that w_M has finite support and $\sum\limits_{v \in F_2} w_M(v) = |M|$. The *$M$-weight* of a vertex $v \in F_2$ is $w_M(v)$. The *interior* of M is the set formed by vertices with M-weight equals 1; the number of interior points in M is denoted by i_M. The *interior boundary* (resp. *exterior boundary*) of M is the set formed by vertices with M-weight equals $1 - ks$ (resp. ks) for some $0 < k \leq 4$. Equivalently, a vertex belongs to the interior of M if it and all its neighbors are contained in M. A vertex belongs to the interior boundary of M if it is contained in M and has at least one neighbor not contained in M. A vertex belongs to the exterior boundary of M if it is not contained in M but has at least one neighbor in M.

Notice that if M is a tree then its exterior boundary contains $2|M| + 2$ elements. Moreover, since the sum of all M-weights equals $|M|$, the interior boundary of a tree has at least $\lceil \frac{2|M|+2}{3} \rceil$ elements and $i_M \leq \lfloor \frac{|M|-2}{3} \rfloor$.

We obtain a non-increasing sequence x_M by ordering the nonzero M-weights. Let $|x_M|$ be the number of terms of x_M. Therefore, if M is a tree then $|x_M| = 3|M|+2$. Given two finite sets of the same cardinality $M_1, M_2 \subset F_2$ we say that $x_{M_1} \geq x_{M_2}$ if the sum of the first n terms of x_{M_1} is greater than or equal to the sum of the first n terms of x_{M_2} for all $1 \leq n \leq \min\{|x_{M_1}|, |x_{M_2}|\}$.

In order to facilitate the reading we write the repeated terms of x_M using exponents. For instance, if $M = \{e, a, a^2, a^3\}$ then x_M has two terms equal to $1 - 2s$, two terms equal to $1 - 3s$ and ten terms equal to s; therefore, we write $x_M = ((1-2s)^2, (1-3s)^2, s^{10})$.

Example 3.2. Consider $m \geq 1$ and let $M_m = \{v_0, v_1, \ldots, v_{m-1}\}$ be the set of the first m words in F_2. Therefore, M is a tree and for $m \leq 5$ we have $x_{M_1} = (1-4s, s^4)$, $x_{M_2} = ((1-3s)^2, s^6)$, $x_{M_3} = ((1-3s)^2, 1-2s, s^8)$, $x_{M_4} = ((1-3s)^3, 1-s, s^{10})$ and $x_{M_5} = (1, (1-3s)^4, s^{12})$.

For $m > 5$ consider $l \geq 1$ and $r \in \{1, 2, \ldots, 4 \cdot 3^l\}$ such that $m = 2 \cdot 3^l - 1 + r$. Notice that for every $k \geq 1$ the words of length k are $v_{2 \cdot 3^{k-1} - 1}, v_{2 \cdot 3^{k-1}}, \ldots, v_{2 \cdot 3^k - 2}$. Thus, $\{v_0, v_1, \ldots, v_{2 \cdot 3^l - 2}\}$ is the set of all words with length at most l. Therefore, an analysis of the three possible values of

$r-3\lfloor\frac{r}{3}\rfloor$ shows that

$$x_{M_m}=(1^{2\cdot 3^{l-1}-1+\lfloor\frac{r}{3}\rfloor},1-s(3-(r-3\lfloor\frac{r}{3}\rfloor)),(1-3s)^{4\cdot 3^{l-1}-1+r-\lfloor\frac{r}{3}\rfloor},s^{4\cdot 3^{l}+2r}).$$

Notice that $1-s(3-(r-3\lfloor\frac{r}{3}\rfloor))\in\{1-s,1-2s,1-3s\}$. $\diamond$

Let $m\geq 1$. We are interested in obtain a subset of F_2 of cardinality m whose corresponding sequence is maximal under the partial order $\geq$. The following lemma shows that such subset must be a tree.

Lemma 3.3. *Let $m\geq 1$ and consider $M\subset F_2$ such that $|M|=m$. Then there exists a tree $\widetilde{M}\subset F_2$ such that $|\widetilde{M}|=m$, $i_{\widetilde{M}}=i_M$ and $x_{\widetilde{M}}\geq x_M$.*

Proof. If M is a tree take $\widetilde{M}=M$. Then, suppose that M is a forest with n connected components $T_1,T_2,\ldots,T_n$. For $k\in\{0,1,2,3\}$, let p_k (resp. q_k) be the number of vertices with M-weight equals $1-(4-k)s$ (resp. $(4-k)s$). Therefore, $x_M=(1^{i_M},(1-s)^{p_3},(1-2s)^{p_2},(1-3s)^{p_1},(1-4s)^{p_0},(4s)^{q_0},(3s)^{q_1},(2s)^{q_2},s^{q_3})$.

For $i\in\{1,2,\ldots,n\}$, denote the exterior boundary of T_i by $\partial_e T_i$. Since there exist no cycles in F_2, we may assume, by possibly relabeling the exterior boundaries, that $\partial_e T_1\cap(\bigcup_{i=2}^{n}\partial_e T_i)$ contains at most one element. Let $w\in M\setminus T_1$ be a word of maximal length. Notice that w is a leaf of one of the connected components of M.

We consider the two possible cases. First, suppose $\partial_e T_1\cap(\bigcup_{i=2}^{n}\partial_e T_i)=\emptyset$. Let M' be the set with $|M|$ elements obtained from M by performing a rigid transformation on T_1 that takes a leaf to a vertex in $F_2\setminus M$ adjacent to w. Thus, $x_{M'}=(1^{i_M},(1-s)^{p_3},(1-2s)^{p_2+2},(1-3s)^{p_1-2},(1-4s)^{p_0},(4s)^{q_0},(3s)^{q_1},(2s)^{q_2},s^{q_3-2})$.

Consider now the case in which $\partial_e T_1\cap(\bigcup_{i=2}^{n}\partial_e T_i)=\{u\}$ for some $u\in F_2$. Thus, u belongs exactly to 2, 3 or 4 exterior boundaries. Suppose that there are distinct numbers $i,j,k\in\{2,3,\ldots,n\}$ such that $\partial_e T_1\cap\partial_e T_i\cap\partial_e T_j\cap\partial_e T_k=\{u\}$, the other cases are similar. Construct M' as in the previous paragraph: perform a rigid transformation on T_1 that takes a leaf to a vertex in $F_2\setminus M$ adjacent to w. Consequently, $x_{M'}=(1^{i_M},(1-s)^{p_3},(1-2s)^{p_2+2},(1-3s)^{p_1-2},(1-4s)^{p_0},(4s)^{q_0-1},(3s)^{q_1+1},(2s)^{q_2},s^{q_3-1})$.

For any of the two cases above, we obtain a set M' such that $|M'|=m$, $i_{M'}=i_M$ and $x_{M'}\geq x_M$. Moreover, M' has $n-1$ connected components. We then obtain $\widetilde{M}$ by repeating the argument above $n-2$ times. ■

Lemma 3.4. *Let $m\geq 5$ and consider $M\subset F_2$ such that $|M|=m$. If $i_M<\lfloor\frac{m-2}{3}\rfloor$ then there exists $\widetilde{M}\subset F_2$ such that $|\widetilde{M}|=m$, $i_{\widetilde{M}}=i_M+1$ and $x_{\widetilde{M}}\geq x_M$.*

Proof. We may assume, by Lemma 3.3, that M is a tree. Thus, there exists no $v \in M$ such that $w_M(v) \in \{1-4s, 4s, 3s, 2s\}$. Let p_1, p_2 and p_3 be the number of vertices in M of degree 1, 2 and 3, respectively. Therefore, it follows that $x_M = (1^{i_M}, (1-s)^{p_3}, (1-2s)^{p_2}, (1-3s)^{p_1}, s^{2m+2})$. For $\delta = \lfloor \frac{m-2}{3} \rfloor - i_M$, since the sum of the M-weights equals m, we have $p_2 + 2p_3 \geq 3\delta$. We consider three cases: $p_2 = 0, p_3 = 0$ and $p_2, p_3 \neq 0$.

First, suppose $p_3 = 0$. Then, $p_2 \geq 3$ and therefore there exist vertices $u, v, w \in M$ of degree 2. Let u_1, u_2 (resp. v_1, v_2) be the vertices in M which are adjacent to u (resp. v). Assume, without loss of generality, that v_2 belongs to the connected component of $M \setminus \{v\}$ that contains u. Analogously, assume that u_2 belongs to the connected component of $M \setminus \{u\}$ that contains v.

Let M' be the set formed by the union of $M \setminus \{u, v\}$ and the two vertices in $F_2 \setminus M$ which are adjacent to w. The tree $\tilde{M}$ with $|M|$ vertices is obtained from M' by performing two rigid transformations; Figure 3.1 shows two examples of this construction. The first transformation is performed on the connected component of M' that contains u_1, and takes u_1 to u. The second transformation is performed on the connected component of M' that contains v_1, and takes v_1 to v. Thus, $x_{\widetilde{M}} = (1^{i_M+1}, (1-s)^{p_3}, (1-2s)^{p_2-3}, (1-3s)^{p_1+2}, s^{2m+2})$.

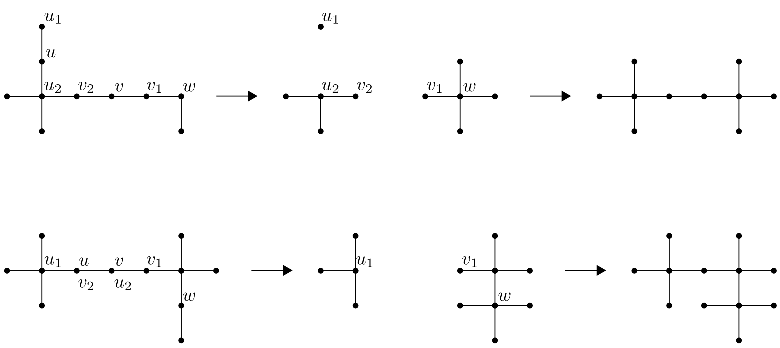

Figure 3.1: Two examples of a tree M with $p_3 = 0$ and the construction of $\widetilde{M}$.

Suppose $p_3 \neq 0$ and $p_2 \neq 0$. Then there exist vertices $u, v \in M$ of degree 2 and degree 3, respectively. Let M' be the union of $M \setminus \{u\}$ and the vertex in $F_2 \setminus M$ which is adjacent to v. Now, as in the previous paragraph, obtain a tree $\widetilde{M}$ by performing a rigid transformation; Figure 3.2 below shows an example of this construction. Thus, $x_{\widetilde{M}} = (1^{i_M+1}, (1-s)^{p_3-1}, (1-2s)^{p_2-1}, (1-3s)^{p_1+1}, s^{2m+2})$.

Finally, suppose $p_2 = 0$. Then, $p_3 \geq 2$ and there exist vertices $u, v \in M$ of degree 3. Let u_1 (resp. v_1) be the vertex adjacent to u (resp. v) not contained in M.

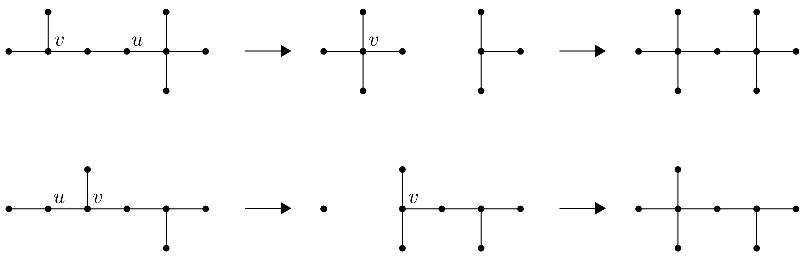

Figure 3.2: Examples of a tree M with $p_3, p_2 \neq 0$ and the construction of $\widetilde{M}$.

We may assume that u is adjacent to a leaf. If not, since every vertex adjacent to a leaf has degree at least 3, there exist leaves l_1 and l_2 adjacent to a vertex of degree 4. Therefore, $(M \setminus \{l_1\}) \cup \{u_1\}$ contains a vertex of degree 3, which is adjacent to a leaf, and its corresponding sequence equals x_M.

Let $\widetilde{M}$ be the set obtained from $M \cup \{v_1\}$ by removing the leaf contained in M which is adjacent to u; Figure 3.3 shows an example of this construction. Notice that $x_{\widetilde{M}} = (1^{i_M+1}, (1-s)^{p_3-2}, (1-2s)^{p_2+1}, (1-3s)^{p_1}, s^{2m+2})$.

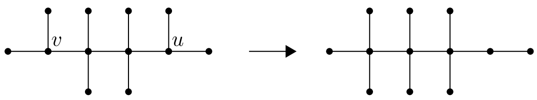

Figure 3.3: A tree M and the set $\widetilde{M}$.

Therefore, for any of the three possible cases above, we obtain a tree $\widetilde{M}$ with m vertices. Moreover, notice that $i_{\widetilde{M}} = i_M + 1$ and $x_{\widetilde{M}} \geq x_M$. ∎

Lemma 3.5. *Consider $m \geq 1$ and let $M_m = \{v_0, v_1, \dots, v_{m-1}\}$ be the set of the first m words in F_2. If $M \subset F_2$ is such that $|M| = m$ then $x_{M_m} \geq x_M$.*

Proof. We may assume, by Lemma 3.3, that M is a tree. If $m \leq 5$ the result then follows by checking a few cases. If $m > 5$ then $m = 2 \cdot 3^l - 1 + r$ for some $l \geq 1$ and $r \in \{1, 2, \dots, 4 \cdot 3^l\}$. Therefore, as in Example 3.2, we have that $x_{M_m} = (1^{2\cdot 3^{l-1}-1+\lfloor \frac{r}{3} \rfloor}, 1 - s(3 - (r - 3\lfloor \frac{r}{3} \rfloor)), (1-3s)^{4\cdot 3^{l-1}-1+r-\lfloor \frac{r}{3} \rfloor}, s^{4\cdot 3^l + 2r})$.

By Lemma 3.4, it is sufficient to consider the case $i_M = \lfloor \frac{m-2}{3} \rfloor$. Let p_2 (resp. p_3) be the number of vertices in M of degree 2 (resp. 3). Since the sum of the terms of x_M equals m, it follows that $\frac{m-2-(p_2+2p_3)}{3} = \lfloor \frac{m-2}{3} \rfloor$. Therefore, $r - 3\lfloor \frac{r}{3} \rfloor = p_2 + 2p_3$ and $(p_2, p_3) \in \{(0,0), (1,0), (2,0), (0,1)\}$. If $(p_2, p_3) \in \{(0,0), (1,0), (0,1)\}$ then x_M equals x_{M_m}. If $(p_2, p_3) = (2,0)$ then $x_{M_m} \geq x_M$. ∎

Let $(X_t)_{t \geq 1}$ be a sequence of i.i.d. random variables which assume values in F_2 such that $\mathbb{P}(X_1 = a) = \mathbb{P}(X_1 = b) = \mathbb{P}(X_1 = a^{-1}) = \mathbb{P}(X_1 = b^{-1}) = s$ and $\mathbb{P}(X_1 = e) = 1 - 4s$. We denote by $P(n,t)$ the probability that $X_1 X_2 \dots X_t$ equals v_n. For instance, $P(0,1) = 1 - 4s$, $P(0,2) = (1-4s)^2 + 4s^2$ and

$P(0,3) = (1-4s)((1-4s)^2+12s^2)$. Notice that $P(n,t) \geq P(n+1,t)$ for every $n \geq 0$.

Let $y_0, y_1, \ldots y_t$ be fixed but arbitrary elements in F_2 and consider the random variable $Z = y_0X_1y_1\ldots X_ty_t$. We denote by $Q(n,t)$ the probability that Z equals v_n. The following lemma compares the probabilities $P(n,t)$ and $Q(n,t)$.

Lemma 3.6. *Let $t \geq 0$ and $m \geq 1$. If $n_0, n_1, \ldots, n_{m-1} \in \mathbb{N}$ are distinct then $Q(n_0,t)+Q(n_1,t)+\ldots+Q(n_{m-1},t) \leq P(0,t)+P(1,t)+\ldots+P(m-1,t)$.*

Proof. The proof is by induction on t. The case $t=0$ follows trivially, since $P(0,0) = 1$. It suffices to prove the result for $Z = X_1y_1\ldots X_{t-1}y_{t-1}X_t$. Indeed, the general case then follows by considering the distinct numbers $k_0, k_1, \ldots, k_{m-1}$ such that $v_{k_i} = y_0^{-1}v_{n_i}y_t^{-1}$ for all $0 \leq i \leq m-1$. Let $Z' = X_1y_1\ldots X_{t-1}y_{t-1}$ and define the two finite sets $M = \{v_{n_0}, v_{n_1}, \ldots, v_{n_{m-1}}\}$ and $M_m = \{v_0, v_1, \ldots, v_{m-1}\}$. Let $j > m$ be such that $v_{n_m}, v_{n_{m+1}}, \ldots v_{n_j}$ are the elements in the exterior boundary of M. Suppose, without loss of generality, that $w_M(v_{n_k}) \geq w_M(v_{n_{k+1}})$ for all $k \leq j-1$.

Notice that $\sum\limits_{i=0}^{m-1} Q(n_i,t) = \mathbb{P}(Z \in M) = \sum\limits_{i=0}^{j} \mathbb{P}(Z' = v_{n_i})w_M(v_{n_i})$. By the induction hypothesis,

$$\begin{aligned}\sum_{i=0}^{j}\mathbb{P}(Z'=v_{n_i})w_M(v_{n_i}) &= \sum_{i=0}^{j}\Big(\sum_{k\leq i}\mathbb{P}(Z'=v_{n_k})\Big)(w_M(v_{n_i})-w_M(v_{n_{i+1}})) \\ &\leq \sum_{i=0}^{j}\Big(\sum_{k\leq i}P(k,t-1)\Big)(w_M(v_{n_i})-w_M(v_{n_{i+1}})) \qquad (5.1)\end{aligned}$$

On the other hand, Equation 5.1 equals

$$\sum_{i=0}^{j}P(i,t-1)w_M(v_{n_i}) = \sum_{i=0}^{j}\Big(\sum_{k\leq i}w_M(v_{n_k})\Big)(P(i,t-1)-P(i+1,t-1))$$

and therefore, by Lemma 3.5, less than or equal to

$$\sum_{i=0}^{j}\Big(\sum_{k\leq i}w_{M_m}(v_k)\Big)(P(i,t-1)-P(i+1,t-1)). \qquad (5.2)$$

The result then follows by noticing that Equation 5.2 equals

$$\sum_{i=0}^{j}w_{M_m}(v_i)P(i,t-1) = \mathbb{P}(X_1X_2\ldots X_t \in M_m) = \sum_{i=0}^{m-1}P(i,t).$$

■

As a corollary, we obtain Lemma 3.1.

Proof of Lemma 3.1. The first part of the desired result follows from Lemma 3.6 by setting $m = 1$ and $n_0 = 0$. For the second part, by the Varopoulos-Carne bound (see, e.g., Theorem 13.4 of [14]), we obtain a constant $\alpha \in (0,1)$ such that $\mathbb{P}(X_1 \dots X_t = e) \le \alpha^t$ for all $t \ge 0$. ∎

3.2
Proof of Theorem 1.1

Let $N_0 \in \mathbb{N}$ and consider a set of tilings $\mathcal{B} \subseteq \mathcal{T}(\mathcal{R}_{N_0})$. We say that a tiling $\mathbf{t}$ of a cork $\mathcal{R}_{N_1,N_2;p_1,p_2}$ is formed by (k,M)-blocks of $\mathcal{B}$ if there exist distinct nonnegative integers $b_1 < b_2 < \dots < b_k$ and tilings $\mathbf{b}_1, \mathbf{b}_2, \dots, \mathbf{b}_k \in \mathcal{B}$ such that, for each $M_j = b_j(2M + N_0) + M + N_1$, the restriction of $\mathbf{t}$ to $\mathcal{D} \times [M_j, M_j + N_0]$ equals $\mathbf{b}_j$. In other words, there are k specific subregions in $\mathbf{t}$, located at positions determined by N_0 and M, where $\mathbf{t}$ coincides with a tiling contained in $\mathcal{B}$.

We denote by $\operatorname{block}_{\mathcal{B}}^M(\mathbf{t})$ the maximum nonnegative integer k such that $\mathbf{t}$ is formed by (k,M)-blocks of $\mathcal{B}$. The following lemma shows that $\operatorname{block}_{\mathcal{B}}^M(\mathbf{t})$ is almost never very small. More precisely, except with exponentially small probability, a uniform random tiling of $\mathcal{D}\times[0,N]$ contains linearly many blocks. The proof uses the result from [21] stated below.

Fact 3.7 (Lemma 13 of [21])**.** *Given a quadriculated region $\mathcal{D} \subset \mathbb{R}^2$ there exist $\lambda_1 > 0, c \in (0,1)$ and a unit vector $v_1 \in \mathbb{R}^{\mathcal{P}}$ with positive coordinates such that (when $N \to \infty$)*

$$|\mathcal{T}(\mathcal{R}_{0,N;p,\tilde{p}})| = (v_1)_p (v_1)_{\tilde{p}} \lambda_1^N (1 + o(c^N)).$$

Furthermore, for all $\epsilon > 0$ there exists $N_\epsilon \in \mathbb{N}$ such that if $p_0, p_N \in \mathcal{P}, j > N_\epsilon, N > j + N_\epsilon$ and $\mathbf{T}$ is a random tiling of $\mathcal{R}_{0,N;p_0,p_N}$ then

$$(v_1)_p^2 - \epsilon < \mathbb{P}(\operatorname{plug}_j(\mathbf{T}) = p) < (v_1)_p^2 + \epsilon.$$

Lemma 3.8. *Consider a quadriculated disk $\mathcal{D}$, $N_0 \in \mathbb{N}$ and $\mathcal{B} \subseteq \mathcal{T}(\mathcal{R}_{N_0})$. There exist $M \in 2\mathbb{N}$ and constants $c, \tilde{c} \in (0,1)$ such that the following holds. If $\mathbf{T}_N$ is a random tiling of $\mathcal{R}_N$ with $N > N_0$ then* $\mathbb{P}(\operatorname{block}_{\mathcal{B}}^M(\mathbf{T}_N) < \tilde{c}N) = o(c^N)$.

Proof. Recall that $\mathbf{p}_\circ$ is the empty plug. By Fact 3.7, there exist $\epsilon > 0$ and an even integer $N_\epsilon \ge |\mathcal{D}|$ such that if $j \ge N_\epsilon$, $\tilde{N} \ge j + N_\epsilon$ and $p_0, p_{\tilde{N}} \in \mathcal{P}$ then, for a random tiling $\tilde{\mathbf{T}}$ of $\mathcal{R}_{0,\tilde{N};p_0,p_{\tilde{N}}}$, we have $\mathbb{P}(\operatorname{plug}_j(\tilde{\mathbf{T}}) = \mathbf{p}_\circ) > \epsilon$. Let $m = \max_{p_i,p_j \in \mathcal{P}} |\mathcal{T}(\mathcal{R}_{0,N_\epsilon;p_i,\mathbf{p}_\circ})||\mathcal{T}(\mathcal{R}_{0,N_\epsilon+N_0;\mathbf{p}_\circ,p_j})|$ and $\delta = \epsilon|\mathcal{B}|m^{-1}$. We claim that if $\tilde{N} = 2N_\epsilon + N_0$ then $\mathbb{P}(\operatorname{block}_{\mathcal{B}}^{N_\epsilon}(\tilde{\mathbf{T}}) \ge 1) > \delta$.

Since $N_\epsilon \geq |\mathcal{D}|$, by Remark 2.2, there exist tilings $\mathbf{t}_1$ of $\mathcal{R}_{0,N_\epsilon,p_0,\mathbf{p}_\circ}$ and $\mathbf{t}_2$ of $\mathcal{R}_{0,N_\epsilon,\mathbf{p}_\circ,p_{\tilde{N}}}$. Thus, each tiling $\mathbf{b}$ in $\mathcal{B}$ defines a tiling $\tilde{\mathbf{t}} = \mathbf{t}_1 * \mathbf{b} * \mathbf{t}_2$ of the cork $\mathcal{R}_{0,\tilde{N};p_0,p_{\tilde{N}}}$ with $\operatorname{plug}_{N_\epsilon}(\tilde{\mathbf{t}}) = \mathbf{p}_\circ$ and $\operatorname{block}^{N_\epsilon}_{\mathcal{B}}(\tilde{\mathbf{t}}) = 1$. Moreover, notice that the number of tilings of $\mathcal{R}_{0,\tilde{N},p_0,p_{\tilde{N}}}$ such that the N_ϵ-th plug equals $\mathbf{p}_\circ$ is smaller than m. Therefore, $\mathbb{P}(\operatorname{block}^{N_\epsilon}_{\mathcal{B}}(\tilde{\mathbf{T}}) \geq 1 \mid \operatorname{plug}_{N_\epsilon}(\tilde{\mathbf{T}}) = \mathbf{p}_\circ) \geq |\mathcal{B}|m^{-1}$ and the claim above is proved.

Take $M = N_\epsilon$ and $\tilde{c} = \frac{\delta}{2(2M+N_0)}$. For each $i = 1, 2, \ldots, \left\lfloor \frac{N}{2M+N_0} \right\rfloor$ let A_i be the event that the restriction of $\mathbf{T}_N$ to $\mathcal{D} \times [(i-1)(2M+N_0), i(2M+N_0)]$ is formed by $(1, M)$-blocks of $\mathcal{B}$. Notice that the previous paragraph implies that $\mathbb{P}(A_i \mid \mathbf{T}_N$ constructed up to floor $(i-1)(2M+N_0)) > \delta$. Therefore, we have that $\mathbb{P}(\operatorname{block}^M_{\mathcal{B}}(\mathbf{T}_N) < \tilde{c}N) \leq \mathbb{P}(X < \tilde{c}N)$ where X is a random variable with binomial distribution $\operatorname{Bin}(\left\lfloor \frac{N}{2M+N_0} \right\rfloor, \delta)$. By writing X as a sum of i.i.d. random variables with Bernoulli distribution $\operatorname{Bern}(\delta)$, the result follows from Chernoff's inequality. ■

We are now ready to prove Theorem 1.1.

Proof of Theorem 1.1. Let $\phi\colon G^+_{\mathcal{D}} \to F_2$ be a surjective homomorphism. Consider $N_0 \in 2\mathbb{N}$ sufficiently large so that there exist tilings $\mathbf{b}_a$ and $\mathbf{b}_b$ of $\mathcal{R}_{N_0}$ with $\phi(\mathbf{b}_a) = a$ and $\phi(\mathbf{b}_b) = b$. Let $\mathbf{b}_{e_1}$ be the tiling $\mathbf{t}_{\mathrm{vert},N_0}$. We obtain four distinct tilings $\mathbf{b}_{e_2}, \mathbf{b}_{e_3}, \mathbf{b}_{e_4}, \mathbf{b}_{e_5}$ from $\mathbf{b}_{e_1}$ by performing exactly one vertical flip. Define the set $\mathcal{B} = \{\mathbf{b}_a, \mathbf{b}_a^{-1}, \mathbf{b}_b, \mathbf{b}_b^{-1}, \mathbf{b}_{e_1}, \mathbf{b}_{e_2}, \mathbf{b}_{e_3}, \mathbf{b}_{e_4}, \mathbf{b}_{e_5}\} \subset \mathcal{T}(\mathcal{R}_{N_0})$. Set $s = \frac{1}{9}$ (importantly, $s \in (0, \frac{1}{8})$ and we will be able to use Lemma 3.1 later). We have $|\mathcal{B} \cap \phi^{-1}(\{x\})| = s|\mathcal{B}|$ for every $x \in \{a, a^{-1}, b, b^{-1}\}$ and $|\mathcal{B} \cap \phi^{-1}(\{e\})| = (1-4s)|\mathcal{B}|$. By Lemma 3.8, there exist $M \in 2\mathbb{N}$ and $\tilde{c} \in (0,1)$ such that the probability that $\operatorname{block}^M_{\mathcal{B}}(\mathbf{T}_i)$ is smaller than $r = \lceil \tilde{c}N \rceil$ goes to zero exponentially. We may therefore assume that $\mathbf{T}_1$ and $\mathbf{T}_2$ are formed by at least (r, M)-blocks of $\mathcal{B}$.

Let $\mathcal{B}_r(\mathcal{R}_N) \subset \mathcal{T}(\mathcal{R}_N)$ be the set of tilings of $\mathcal{R}_N$ formed by at least (r, M)-blocks of $\mathcal{B}$. For each tiling $\mathbf{t} \in \mathcal{B}_r(\mathcal{R}_N)$ let $b_{1,\mathbf{t}} < b_{2,\mathbf{t}} < \ldots < b_{r,\mathbf{t}}$ be the first r nonnegative integers such that, for $j = 1, 2, \ldots, r$ and $M_{j,\mathbf{t}} = b_{j,\mathbf{t}}(2M+N_0) + M$, the restriction of $\mathbf{t}$ to $\mathcal{D} \times [M_{j,\mathbf{t}}, M_{j,\mathbf{t}} + N_0]$ equals a tiling in $\mathcal{B}$. We now define an equivalence relation $\approxeq$ on $\mathcal{B}_r(\mathcal{R}_N)$: $\tilde{\mathbf{t}} \approxeq \hat{\mathbf{t}}$ if and only if $b_{j,\tilde{\mathbf{t}}} = b_{j,\hat{\mathbf{t}}}$ (for all j) and $\tilde{\mathbf{t}}$ equals $\hat{\mathbf{t}}$ in the region $(\mathcal{D} \times [0, N]) \smallsetminus (\bigcup_{j=1}^r \mathcal{D} \times [M_{j,\tilde{\mathbf{t}}}, M_{j,\tilde{\mathbf{t}}} + N_0])$.

Let $B_1, B_2, \ldots, B_l$ be the $\approxeq$-equivalence classes. Notice that, for each $i \leq l$, there are fixed tilings $\mathbf{t}_{0,i}, \mathbf{t}_{1,i}, \ldots, \mathbf{t}_{r,i}$ such that B_i consists of all tilings of the form $\mathbf{t}_{0,i} * \mathbf{b}_1 * \mathbf{t}_{1,i} * \mathbf{b}_2 * \mathbf{t}_{3,i} * \ldots * \mathbf{b}_r * \mathbf{t}_{r,i}$ with $\mathbf{b}_1, \mathbf{b}_2, \ldots, \mathbf{b}_r \in \mathcal{B}$. Thus, each $\approxeq$-equivalence class has size exactly $|\mathcal{B}|^r$.

Suppose that $\mathbf{T}_1$ has been chosen first from $\mathcal{B}_r(\mathcal{R}_N)$, say $\mathbf{T}_1 = \mathbf{t}$. The probability that there exists a sequence of flips joining $\mathbf{T}_2$ and $\mathbf{t}$ is less than or equal to the probability that ϕ takes $\mathbf{T}_2 * \mathbf{t}^{-1}$ to the identity, as ϕ is a homomorphism. We prove that the later probability decays exponentially with N. To this end, it suffices to show that the conditional probabilities $\mathbb{P}(\phi(\mathbf{T}_2 * \mathbf{t}^{-1}) = e \mid \mathbf{T}_2 \in B_i)$ are uniformly bounded in i by α^r for some constant $\alpha \in (0,1)$.

Consider a sequence $(X_t)_{t\geq 1}$ of i.i.d. random variables in F_2 such that $\mathbb{P}(X_1 = e) = 1 - 4s$ and $\mathbb{P}(X_1 = x) = s$ for $x \in \{a, a^{-1}, b, b^{-1}\}$. By construction, $\mathbb{P}(\phi(\mathbf{T}_2 * \mathbf{t}^{-1}) = e \mid \mathbf{T}_2 \in B_i) = \mathbb{P}(\phi(\mathbf{t}_{0,i}) X_1 \phi(\mathbf{t}_{1,i}) \dots X_r \phi(\mathbf{t}_{r,i} * \mathbf{t}^{-1}) = e)$. The result now follows from Lemma 3.1. ■

4
The domino group of thin rectangles

In this section we prove Theorem 1.3, that is, we compute the even domino group of $\mathcal{D}_L = [0, L] \times [0, 2]$ for $L \geq 3$. The strategy consists in constructing a homomorphism from $G^+_{\mathcal{D}_L}$ to the group G^+_L defined in Equation 1.1. We then prove that this homomorphism is in fact an isomorphism.

The computation of $G^+_{\mathcal{D}_L}$ is inspired by the results of [19], where a flip invariant for tilings of duplex regions is exhibited. By performing a rotation, we think of tilings of $\mathcal{D}_L \times [0, N]$ as tilings of the duplex region $[0, N] \times [0, L] \times [0, 2]$. Therefore, in this section, we say that a flip is horizontal if it is performed in two dominoes contained in one of the two floors of the new rotated tiling; the flip is vertical otherwise.

Let $\mathbf{t}$ be a tiling of $\mathcal{D}_L \times [0, N]$ and orient each domino contained in $\mathbf{t}$ from its white unit cube to its black unit cube. By projecting the two floors of $\mathbf{t}$ on the plane $z = 0$, we obtain a *diagram* $\mathcal{I}_{\mathbf{t}}$ on $[0, N] \times [0, L]$ containing oriented disjoint cycles and *jewels*, i.e., unit squares formed by the projections of dominoes parallel to the z-axis. A cycle is *trivial* if it has length two and a jewel is *trivial* if it is not enclosed by a cycle. The color of a jewel j is defined as the color of its corresponding unit square in the rectangle $[0, N] \times [0, L]$. We write $\operatorname{color}(j) = +1$ if j is white and $\operatorname{color}(j) = -1$ if j is black. The Figure 4.1 shows an example of a tiling and its associated diagram; we always exhibit trivial cycles in green, counterclockwise cycles in red and clockwise cycles in blue.

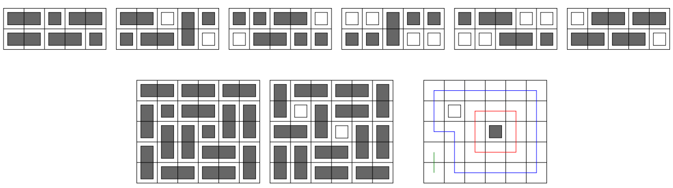

Figure 4.1: The first row shows a tiling $\mathbf{t}$ of $\mathcal{D}_5 \times [0, 6]$. The second row shows $\mathbf{t}$ after a rotation and its diagram $\mathcal{I}_{\mathbf{t}}$.

We order the jewels contained in $\mathcal{I}_{\mathbf{t}}$. Let $j_1 = [a, a+1] \times [b, b+1]$ and $j_2 = [c, c+1] \times [d, d+1]$ be two jewels. If j_1 and j_2 are in different columns, i.e. $a \neq c$, we write $j_1 < j_2$ if $a < c$. If j_1 and j_2 are in the same column, i.e. $a = c$, we write $j_1 < j_2$ if $b > d$. When this order is used, jewels are called *ordered jewels.*

For a jewel j let $\operatorname{wind}(j)$ be the sum of the winding numbers around j over all the cycles in $\mathcal{I}_{\mathbf{t}}$. Notice that $\operatorname{wind}(j)$ is an integer and $|\operatorname{wind}(j)| \leq \left\lfloor \frac{L-1}{2} \right\rfloor$. We are especially interested in the winding numbers of jewels contained in the same column. Consider the set $R_L = \{(m,n) \in \mathbb{Z}^2 \colon \max\{|m|,|n|,|m-n|\} < \lfloor \frac{L}{2} \rfloor\}$. Figure 4.2 below shows the elements of R_{10} and two tilings of $\mathcal{D}_{10} \times [0,12]$, notice that in the figure any two jewels j_1 and j_2 contained in the same column are such that $(\mathrm{wind}(j_1), \mathrm{wind}(j_2)) \in R_{10}$.

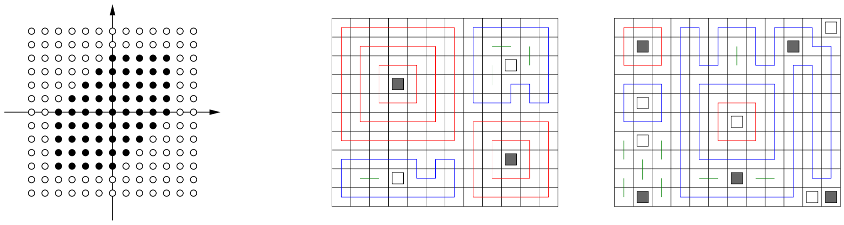

Figure 4.2: The square lattice with elements of R_{10} shown in black, and two diagrams of tilings of $\mathcal{D}_{10} \times [0,12]$.

Lemma 4.1. *Consider $L \geq 3$. Then $(m,n) \in R_L$ if and only if there exist $N \in \mathbb{N}$ and a tiling $\mathbf{t}$ of $\mathcal{D}_L \times [0,2N]$ such that $\mathcal{I}_{\mathbf{t}}$ contains two jewels j_1 and j_2 in the same column with* $(\mathrm{wind}(j_1), \mathrm{wind}(j_2)) = (m,n)$.

Proof. We first prove the *if* direction. Suppose that $j_1 = [a,a+1] \times [b,b+1]$ and $j_2 = [a,a+1] \times [c,c+1]$ with $b > c$. Since $\mathrm{wind}(j_1) = m$ there exists at least $|m|$ unit squares in $[a,a+1] \times [b+1,L]$. Analogously, there exists at least $|n|$ unit squares in $[a,a+1] \times [0,c]$. Moreover, we must have at least $|m-n|$ cycles not enclosing both jewels. Therefore, there exists at least $|m-n|$ unit squares in $[a,a+1] \times [b+1,c]$. Then, $|m|+|n|+|m-n| \leq L-2$ and we have $\max\{|m|,|n|,|m-n|\} \leq \frac{L-2}{2}$.

For the *only if* direction let $(m,n) \in R_L$ and take N sufficiently large. In order to show the existence of a tiling $\mathbf{t}$ of $\mathcal{D}_L \times [0,2N]$ with the desired properties we proceed backwards. Indeed, since a tiling is entirely determined by its diagram, it suffices to construct $\mathcal{I}_{\mathbf{t}}$.

We first deal with the case in which $|m|+|n| < \lfloor \frac{L}{2} \rfloor$. Consider two disjoint squares centered in the same column: s_m of side $2|m|+1$ and s_n of side $2|n|+1$. Let the jewel j_1 (resp. j_2) be the center of s_m (resp. s_n). Construct $|m|$ cycles in s_m and $|n|$ cycles in s_n such that $\mathrm{wind}(j_1) = m$ and $\mathrm{wind}(j_2) = n$. Now, to obtain $\mathcal{I}_{\mathbf{t}}$, fill the rest of $[0,2N] \times [0,L]$ with trivial cycles and trivial jewels.

We are left with the case $|m|+|n| \geq \lfloor \frac{L}{2} \rfloor$, so that $\mathrm{sign}(m) = \mathrm{sign}(n)$. Suppose that $|m| \geq |n|$ and write $|n| = |m| - r$, where $0 \leq r \leq |m|$. The square $s = [0, 2|m|+2]^2$ is contained in $[0,2N] \times [0,L]$, since $|m| < \lfloor \frac{L}{2} \rfloor$. Let $j_1 = [|m|,|m|+1] \times [|m|+1,|m|+2]$ and $j_2 = [|m|,|m|+1] \times [|m|-r,|m|-r+1]$. Construct m cycles in s such that $\mathrm{wind}(j_1) = m$. We have $\mathrm{wind}(j_2) = n$, as $\mathrm{sign}(m) = \mathrm{sign}(n)$. The result then follows by proceeding as in the previous paragraph. ■

Recall that, as in Equation 1.1, $G_L^+ = \langle S_L \mid [a_m, a_n] = 1 \text{ for } (m,n) \in R_L \rangle$, where $S_L = \{a_i : i \in \mathbb{Z}_{\neq 0} \text{ and } |i| \leq \lfloor \frac{L-1}{2} \rfloor\}$. We construct a map

$$\Phi\colon \bigcup_{N \geq 1} \mathcal{T}(\mathcal{D}_L \times [0, 2N]) \to G_L^+.$$

Consider a tiling $\mathbf{t}$ of $\mathcal{D}_L \times [0, 2N]$ and let $j_1 < j_2 < \ldots < j_k$ be the ordered jewels in $\mathcal{I}_{\mathbf{t}}$. Define $\Phi(\mathbf{t}) = b_1 \ldots b_k$ where $b_i = a_{\mathrm{wind}(j_i)}^{\mathrm{color}(j_i)}$ if $\mathrm{wind}(j_i) \neq 0$ and $b_i = e$ if $\mathrm{wind}(j_i) = 0$.

Lemma 4.2. *The map Φ induces a homomorphism $\phi\colon G_{\mathcal{D}_L}^+ \to G_L^+$.*

Proof. Notice that Φ preserves the group operation, given by concatenation of tilings, as a consequence of the ordering of the jewels and the definition of Φ. Thus, it suffices to check that Φ is invariant under flips. Let $\mathbf{t}$ be a tiling of $\mathcal{D}_L \times [0, 2N]$. Consider a horizontal flip performed in two dominoes d_1 and d_2. The horizontal flip either connects two disjoint cycles or disconnects a cycle into two cycles. Suppose the former, the other case is similar. Therefore, d_1 and d_2 are contained in distinct cycles. If either d_1 or d_2 is contained in a trivial cycle then it is easy to see that the horizontal flip does not change the winding number of any jewel. Then, suppose that d_1 and d_2 are contained in nontrivial cycles, Figure 4.3 shows an example of the possible cases.

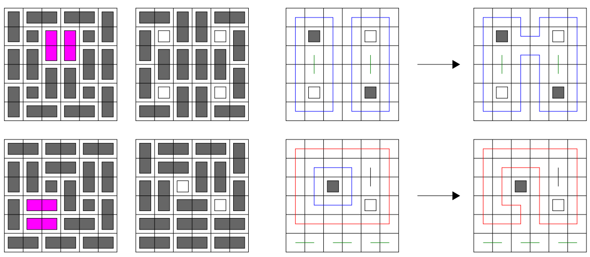

Figure 4.3: Two tilings and the effect of a horizontal flip (highlighted in magenta) on their diagrams.

If d_1 and d_2 are contained in cycles having the same orientation then the flip connects the two cycles preserving the orientation. If d_1 and d_2 are contained in cycles having opposite orientations then one cycle must be enclosed by the other. The flip then creates a cycle with the same orientation as the outer cycle. Moreover, the new cycle encloses only jewels enclosed by the outer cycle but not by the inner cycle. Therefore, in any of the possible cases, the flip preserves the winding number of the jewels. Then, Φ is invariant under horizontal flips.

Consider a vertical flip that takes a trivial cycle to two adjacent jewels (i.e., jewels whose corresponding unit squares are adjacent); a similar analysis holds for the reverse of this flip. The flip creates adjacent jewels j and j' such that $j < j'$, $\operatorname{wind}(j) = \operatorname{wind}(j')$ and $\operatorname{color}(j) \neq \operatorname{color}(j')$. If j and j' are in the same column then the flip clearly preserves the value of $\Phi(\mathbf{t})$. Otherwise, the definition of G_L^+ and Lemma 4.1 imply that the contributions of jewels between j and j' commute so that Φ is invariant under vertical flips. ■

Our objective is to prove that the homomorphism ϕ obtained above is an isomorphism. To achieve this, we now study the even domino group $G^+_{\mathcal{D}_L}$. We follow [19] to derive a family of generators of $G^+_{\mathcal{D}_L}$. A tiling $\mathbf{t}$ of $\mathcal{D}_L \times [0, N]$ is called a *boxed tiling* if its corresponding diagram $\mathcal{I}_\mathbf{t}$ is composed of a nontrivial jewel j and trivial jewels outside the square of center j and side $2|\operatorname{wind}(j)|+1$.

We prefer to work with boxed tilings due to some helpful properties. Notably, we can move via flips the nontrivial jewel of a boxed tiling so that the resulting tiling is a boxed tiling as well. Specifically, consider two boxed tilings $\mathbf{t}$ and $\tilde{\mathbf{t}}$ of $\mathcal{D}_L \times [0, N]$. Let j and $\tilde{j}$ be the nontrivial jewels of $\mathcal{I}_\mathbf{t}$ and $\mathcal{I}_{\tilde{\mathbf{t}}}$, respectively. If $\operatorname{color}(j) = \operatorname{color}(\tilde{j})$ and $\operatorname{wind}(j) = \operatorname{wind}(\tilde{j})$ then $\mathbf{t} \approx \tilde{\mathbf{t}}$. For instance, Figure 4.4 shows the process of moving a nontrivial jewel with winding number equals 1. The extension to other cases follows inductively, by initially transforming the outer cycle into a rectangle through flips.

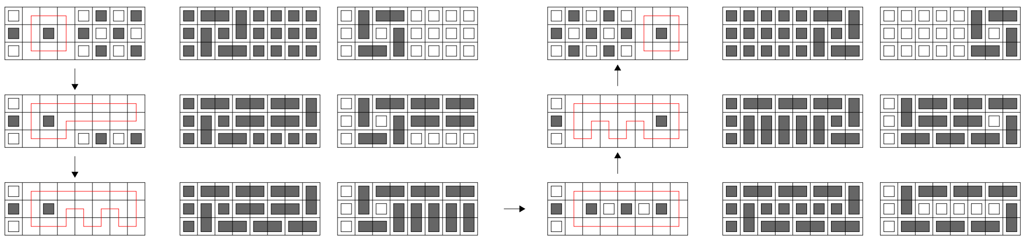

Figure 4.4: The process of moving a nontrivial jewel via a sequence of flips.

The family of boxed tilings generates the even domino group $G^+_{\mathcal{D}_L}$. Indeed, every tiling of a cylinder $\mathcal{D}_L \times [0, 2N]$ is $\sim$-equivalent to a concatenation of boxed tilings.

Lemma 4.3. *Let* $\mathbf{t}$ *be a tiling of* $\mathcal{D}_L \times [0, 2N]$*. Then, there exist* $M \in \mathbb{N}$ *and boxed tilings* $\mathbf{t}_1, \dots, \mathbf{t}_k$ *of* $\mathcal{D}_L \times [0, 2M]$ *such that* $\mathbf{t} \sim \mathbf{t}_1 * \dots * \mathbf{t}_k$.

Proof. This result is proved, in Lemma 7.4 of [19], for diagrams in $\mathbb{Z}^2$ instead of $[0, 2N] \times [0, L]$. However, the same proof holds in our setting, since the relation $\sim$ allows us to assume that N is arbitrarily large. ■

We now investigate relations between boxed tilings. The lemma below shows that, under specific conditions, two boxed tilings commute with respect to concatenation. Notice that the particular case, where the nontrivial jewels of the two boxed tilings share the same color and winding number, follows from the fact that we can move nontrivial jewels.

Lemma 4.4. *Consider boxed tilings* $\mathbf{t}_1$ *of* $\mathcal{D}_L \times [0, 2N_1]$ *and* $\mathbf{t}_2$ *of* $\mathcal{D}_L \times [0, 2N_2]$. *Let* j_1 *and* j_2 *be the nontrivial jewels in* $\mathcal{I}_{\mathbf{t}_1}$ *and* $\mathcal{I}_{\mathbf{t}_2}$*, respectively. If* $\operatorname{color}(j_1) = \operatorname{color}(j_2)$ *and* $(\operatorname{wind}(j_1), \operatorname{wind}(j_2)) \in R_L$ *then* $\mathbf{t}_1 * \mathbf{t}_2 \approx \mathbf{t}_2 * \mathbf{t}_1$.

Proof. Let $(m, n) = (\operatorname{wind}(j_1), \operatorname{wind}(j_2))$, we focus on the diagram $\mathcal{I}_{\mathbf{t}_1 * \mathbf{t}_2}$. We consider two cases: $|m| + |n| < \lfloor \frac{L}{2} \rfloor$ and $|m| + |n| \geq \lfloor \frac{L}{2} \rfloor$. First suppose the former. This case is a matter of moving the nontrivial jewels (as in Figure 4.4), we proceed in three steps. Initially, move j_1 to a jewel $\widetilde{j_1}$ in $[0, 2N_1] \times [2|n|+1, L]$ and j_2 to a jewel $\widetilde{j_2}$ in $[2N_1, 2(N_1+N_2)] \times [0, 2|n|+1]$. Since $L \geq 2(|m|+|n|+1)$, we can then move $\widetilde{j_1}$ to a jewel $\widehat{j_1}$ in $[2N_2, 2(N_1 + N_2)] \times [2|n| + 1, L]$ and $\widetilde{j_2}$ to a jewel $\widehat{j_2}$ in $[0, 2N_2] \times [0, 2|n| + 1]$. Finally, move $\widehat{j_1}$ (resp. $\widehat{j_2}$) in $[2N_2, 2(N_1 + N_2)] \times [0, L]$ (resp. $[0, 2N_2] \times [0, L]$) to obtain copies of $\mathbf{t}_1$ and $\mathbf{t}_2$. For instance, Figure 4.5 shows a particular case ($L = 6$ and $(m, n) = (1, -1)$) of the general idea.

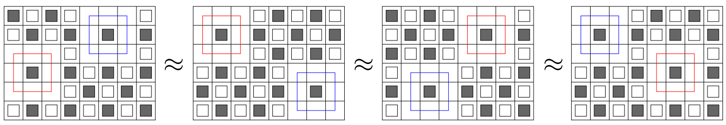

Figure 4.5: The diagram $\mathcal{I}_{\mathbf{t}_1 * \mathbf{t}_2}$ and the effect of three sequences of flips.

We have $R_3 = \{(0, 0)\}, R_4 = \{(0, 0), (\pm 1, 0), (0, \pm 1), (1, 1), (-1, -1)\}$ and $R_5 = R_4$. The previous paragraph cover all cases with the exception of $(m, n) \in \{(1, 1), (-1, -1)\}$ for $L = 4$ and $L = 5$. However, in any of these two cases, the nontrivial jewels share the same color and winding number, so that $\mathbf{t}_1 \approx \mathbf{t}_2$. Therefore, the result holds for $L = 3, 4, 5$.

If $|m|+|n| \geq \lfloor \frac{L}{2} \rfloor$ then $\operatorname{sign}(m) = \operatorname{sign}(n)$. The proof follows by induction on L. Perform a sequence of flips that takes the largest cycle which encloses j_1 to the cycle γ_1 which encloses the region $[1, 2N_1 - 1] \times [1, L - 1]$. Similarly, enlarge the largest cycle which encloses j_2 to obtain the cycle γ_2 which encloses the region $[2N_1 + 1, 2N_1 + 2N_2 - 1] \times [1, L - 1]$. Since $\operatorname{sign}(m) = \operatorname{sign}(n)$ there exists a flip that connects γ_1 and γ_2 into a cycle γ; as before, enlarge γ to obtain a cycle which encloses the region $[1, 2N_1 + 2N_2 - 1] \times [1, L - 1]$.

Now, the winding numbers of j_1 and j_2, when restricted to the region $[1, 2N_1 + 2N_2 - 1] \times [1, L - 1]$, are $m - \operatorname{sign}(m)$ and $n - \operatorname{sign}(n)$, respectively. Notice that $(m - \operatorname{sign}(m), n - \operatorname{sign}(n)) \in R_{L-2}$. Then, by the induction hypothesis, there exists a sequence of flips which commutes the nontrivial jewels in $[1, 2N_1 + 2N_2 - 1] \times [1, L - 1]$. Finally, undo the flips of the previous paragraph to conclude that $\mathbf{t}_1 * \mathbf{t}_2 \approx \mathbf{t}_2 * \mathbf{t}_1$. ∎

We are now ready to prove Theorem 1.3.

Proof of Theorem 1.3. We prove that the homomorphism $\phi \colon G^+_{\mathcal{D}_L} \to G^+_L$ of Lemma 4.2 is an isomorphism. Indeed, we obtain a map $\psi : G^+_L \to G^+_{\mathcal{D}_L}$ such that $\psi^{-1} = \phi$. To this end, we first define a homomorphism $\Psi : F(S_L) \to G^+_{\mathcal{D}_L}$ from the free group generated by S_L to $G^+_{\mathcal{D}_L}$.

Consider a nonzero integer $|i| \leq \left\lfloor \frac{L-1}{2} \right\rfloor$. Let $\mathbf{t}_i$ be the boxed tiling, of the cylinder $\mathcal{D}_L \times [0, 2(|i|+1)]$, such that the nontrivial jewel j_i in $\mathcal{I}_{\mathbf{t}_i}$ is the center of the square $[0, 2|i|+1]^2$ and $\operatorname{wind}(j_i) = i$. Let Ψ be the homomorphism such that $\Psi(a_i) = \mathbf{t}_i$. Then, it follows from Lemma 4.4 that $\Psi(a_m a_n a_m^{-1} a_n^{-1}) = e$ for $(m, n) \in R_L$. Thus, Ψ induces a homomorphism $\psi \colon G^+_L \to G^+_{\mathcal{D}_L}$.

By definition $\phi(\mathbf{t}_i) = a_i$, so that $\phi \circ \psi$ equals the identity map. Now, consider an arbitrary tiling $\mathbf{t}$ of $\mathcal{D}_L \times [0, 2N]$. By Lemma 4.3, $\mathbf{t}$ is $\sim$-equivalent to a concatenation of boxed tilings. Moreover, we know that two boxed tilings whose nontrivial jewels share the same color and winding number are also $\sim$-equivalent. Thus, there exists $i_1, i_2, \ldots, i_k \in \mathbb{Z}$ such that $\mathbf{t} \sim \mathbf{t}_{i_1}^{\epsilon_1} * \mathbf{t}_{i_2}^{\epsilon_2} * \ldots * \mathbf{t}_{i_k}^{\epsilon_k}$ for some $\epsilon_1, \epsilon_2, \ldots, \epsilon_k = \pm 1$. Then, $\phi(\mathbf{t}) = \phi(\mathbf{t}_{i_1}^{\epsilon_1} * \mathbf{t}_{i_2}^{\epsilon_2} * \ldots * \mathbf{t}_{i_k}^{\epsilon_k}) = a_{i_1}^{\epsilon_1} a_{i_2}^{\epsilon_2} \ldots a_{i_k}^{\epsilon_k}$ and therefore $\psi \circ \phi(\mathbf{t}) = \mathbf{t}$. ■

Remark 4.5. We are able to compute the domino group $G_{\mathcal{D}_L}$ once we compute the even domino group $G^+_{\mathcal{D}_L}$. Indeed, consider a tiling $\mathbf{t}_1$ of $\mathcal{D}_L \times [0, 1]$. Then, $\mathbf{t}_1$ is an element of order 2 in $G_{\mathcal{D}_L}$ and generates a subgroup H. Since $\mathbf{t}_1 * \mathbf{t}_1 \approx \mathbf{t}_{\text{vert},2}$, every element in $G_{\mathcal{D}_L}$ is a product of an element in $G^+_{\mathcal{D}_L}$ and an element in H. Thus, the domino group is isomorphic to the inner semidirect product of $G^+_{\mathcal{D}_L}$ and H. More precisely, let $\psi \colon \mathbb{Z}/(2) \to \operatorname{Aut}(G^+_L)$ be the homomorphism defined by $\psi(1)(a_i) = a_{-i}^{-1}$ for each $a_i \in S_L$. Therefore, the semidirect product $\mathbb{Z}/(2) \ltimes_\psi G^+_L$ is isomorphic to the domino group $G_{\mathcal{D}_L}$. ◇

5
Irregular disks

5.1
Non-strongly irregular disks

We show that the family of disks depicted in Figure 1.7 consists of irregular disks that are not strongly irregular. To this end, we rely on concepts from two-dimensional tilings, including the notion of flux introduced in [23], which we briefly recall.

Consider a non-simply connected planar quadriculated region $\mathcal{R}$, so that the topological boundary of $\mathcal{R}$ is not a connected set. A *cut* of $\mathcal{R}$ is an oriented path along the edges of the unit squares in $\mathcal{R}$ that connects a point on the interior boundary to a point on the exterior boundary. The *flux* of a tiling with respect to a cut is defined as the sum of contributions from each domino crossing the cut. A domino contributes $+1$ if its white unit square is to the left of the cut, and -1 if its white unit square is to the right.

For a region $\mathcal{R}$ with n holes, consider n disjoint cuts, each connecting the exterior boundary to a distinct hole, and whose union does not disconnect $\mathcal{R}$. Theorem 1.1 of [23] shows that two tilings of $\mathcal{R}$ can be joined by a sequence of flips if and only if their fluxes with respect to each of the n cuts are equal. For an example, see Figure 5.1.

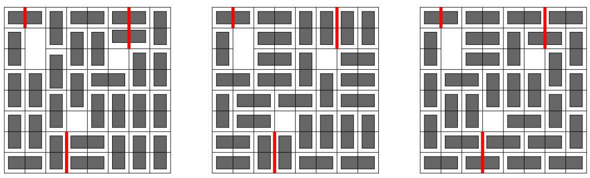

Figure 5.1: Tilings of a non-simply connected planar region with three cuts, represented by red line segments. The first and second (resp. third) tilings have (resp. do not have) the same flux with respect to all three cuts. The first two tilings can be joined through a sequence of flips, while the third tiling cannot be connected to them via flips.

Consider an integer $L \geq 3$. Let $\mathcal{D}_L$ be the disk formed by the union of the rectangle $R_L = [0, 2L] \times [0, 1]$ and the two unit squares $s_0 = [1, 2] \times [-1, 0]$ and $s_L = [2L-2, 2L-1] \times [-1, 0]$; Figure 1.7 exhibits $\mathcal{D}_L$ for $L = 3, 4, 5$. We prove the following result, which implies that $\mathcal{D}_L$ is irregular but not strongly irregular.

Proposition 5.1. *The even domino group $G^+_{\mathcal{D}_L}$ is isomorphic to $\mathbb{Z} \oplus \mathbb{Z}$.*

We first establish a couple of lemmas to obtain two generators of $G^+_{\mathcal{D}_L}$. To this end, we introduce the notion of nontrivial dominoes. Let d_0 and d_L be the dominoes in $\mathcal{D}_L$ that contain s_0 and s_L, respectively. A three-dimensional domino is *nontrivial* if its projection on the xy-plane is equal to either d_0 or d_L.

By removing the nontrivial dominoes and omitting the dominoes contained in $(s_0 \cup s_L) \times [0, 2N]$, a tiling of $\mathcal{D}_L \times [0, 2N]$ can be viewed as a tiling of a planar subregion of $[0, 2L] \times [0, 2N]$; see Figure 5.2 for an example. This perspective allows us to apply results regarding the connectivity under flips of two-dimensional tilings. Notice that the terms horizontal and vertical retain their original sense.

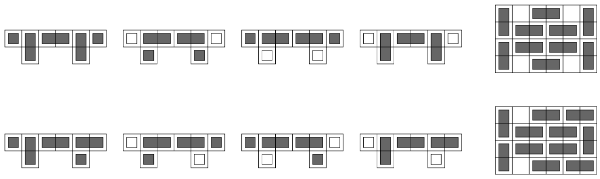

Figure 5.2: Two tilings of $\mathcal{D}_3 \times [0, 4]$ and their depictions in a subregion of $[0, 6] \times [0, 4]$. In this subregion, a domino parallel to the x-axis (resp. y-axis) corresponds to a three-dimensional horizontal (resp. vertical) domino.

Lemma 5.2. *The even domino group $G^+_{\mathcal{D}_L}$ is generated by tilings containing exactly two nontrivial dominoes, which are also nonadjacent.*

Proof. Consider an arbitrary tiling $\mathbf{t}$ of $\mathcal{D}_L \times [0, 2N]$. If $\mathbf{t}$ does not contain nontrivial dominoes then $\mathbf{t}$ can be viewed as a planar tiling of $[0, 2L] \times [0, 2N]$. We then have $\mathbf{t} \approx \mathbf{t}_{\mathrm{vert},2N}$, as any two tilings of a quadriculated disk can be joined by a sequence of flips.

Now, suppose that $\mathbf{t}$ contains nontrivial dominoes. By adding vertical floors and moving some of them downwards (via flips), assume that the first and last floors of $\mathbf{t}$ contain no nontrivial dominoes. Additionally, perform vertical flips to eliminate adjacent nontrivial dominoes.

Notice that, due to the shape of $\mathcal{D}_L$, each nontrivial domino $d \times [K-1, K]$ in $\mathbf{t}$ is accompanied by a vertical domino. Specifically, if $d = d_0$ this vertical domino covers the unit cube $[0, 1]^2 \times [K - 1, K]$, and if $d = d_L$ covers the unit cube $[2L - 1, 2L]^2 \times [K - 1, K]$.

We construct a tiling $\tilde{\mathbf{t}}$ from $\mathbf{t}$ using its 2D perspective as follows; see the first two tilings in Figure 5.3. First, remove all dominoes except the nontrivial dominoes and their accompanying vertical dominoes. Next, tile the remaining part of each punctured 3×3 square centered at a nontrivial domino with three dominoes. Finally, since consecutive nontrivial dominoes are separated by an even number of floors, the remaining region is then tiled by horizontal dominoes in the first and last floors and vertical dominoes elsewhere.

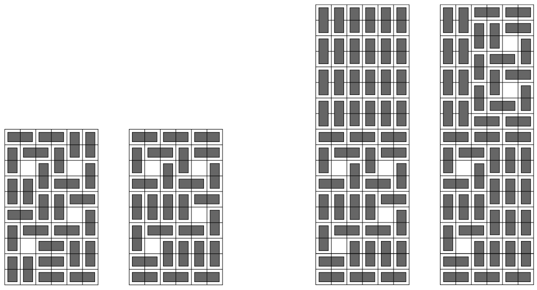

Figure 5.3: The first tiling $\mathbf{t}$ covers $\mathcal{D}_3 \times [0, 10]$. The second tiling $\tilde{\mathbf{t}}$ is constructed from $\mathbf{t}$. The third tiling is obtained from $\tilde{\mathbf{t}}$ by adding vertical floors, a sequence of flips then results in the fourth tiling.

By construction, $\tilde{\mathbf{t}}$ and $\mathbf{t}$ have the same flux with respect to the natural cuts of length one that connect holes defined by the nontrivial dominoes to the exterior boundary. Therefore, we have $\tilde{\mathbf{t}} \approx \mathbf{t}$. Moreover, no domino in $\tilde{\mathbf{t}}$ crosses the line $x = L$, except for certain dominoes in the first and last floors. Consequently, $\tilde{\mathbf{t}}$ is determined by two tilings. Now, by adding vertical floors, shifting one of these two tilings upwards, and performing a few flips after each consecutive pair of nontrivial dominoes, $\tilde{\mathbf{t}}$ decomposes into a concatenation of tilings, each containing exactly two nontrivial dominoes; for an example, see the last two tilings in Figure 5.3. ■

We distinguish eight tilings $\mathbf{t}_{L,1}, \mathbf{t}_{L,2}, \ldots \mathbf{t}_{L,8}$ of $\mathcal{D}_L \times [0, 6]$. For $L = 3$, the two-dimensional perspective of these tilings are illustrated in Figure 5.4. For $L > 3$, the tilings are derived from the case $L = 3$ by translating the dominoes contained in $([4, 6] \times [0, 1] \times [0, 6]) \cup ([4, 5] \times [-1, 0] \times [0, 6])$ by $(2L - 6, 0, 0)$, and adding vertical dominoes in $[4, 2L - 2] \times [0, 1] \times [0, 6]$.

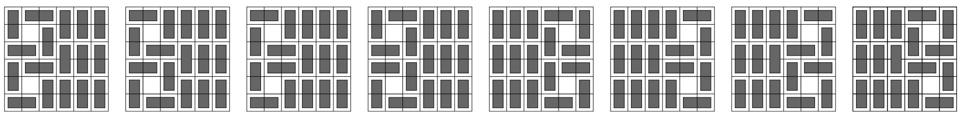

Figure 5.4: The 2D representation of eight tilings of $\mathcal{D}_3 \times [0, 6]$.

Notice that the nontrivial dominoes in $\mathbf{t}_{L,j}$ are separated by two floors. However, this separation can be arbitrarily increased. For any positive even k, let $\mathbf{t}_{L,j,k}$ be the tiling obtained from $\mathbf{t}_{L,j}$ by inserting $k - 2$ vertical floors between the two nontrivial dominoes; in particular, $\mathbf{t}_{L,j,2}$ is equal to $\mathbf{t}_{L,j}$. Thus, $\mathbf{t}_{L,j} \sim \mathbf{t}_{L,j,k}$ and the nontrivial dominoes in $\mathbf{t}_{L,j,k}$ are separated by k floors.

Lemma 5.3. *Let $\mathbf{t}$ be a tiling of $\mathcal{D}_L \times [0, 2N]$ containing exactly two nontrivial dominoes, which are also nonadjacent. There exists j such that $\mathbf{t}_{L,j} \sim \mathbf{t}$.*

Proof. Without loss of generality, assume the nontrivial dominoes in $\mathbf{t}$ are of the form $d_0 \times [K - 1, K]$ and $d_0 \times [M - 1, M]$, with $K < M$. Since these dominoes are not adjacent, we have $M - 1 - K \geq 2$.

Let d and $\tilde{d}$ be the vertical dominoes in $\mathbf{t}$ that cover the unit cubes $[0,1]^2 \times [K-1, K]$ and $[0,1]^2 \times [M-1, M]$, respectively. There are four possible configurations, determined by whether the vertical dominoes covering these unit cubes also cover the adjacent unit cube in the floor above or below. Choose $j \in \{1,2,3,4\}$ such that the translation of d and $\tilde{d}$ by $(0,0,2-K)$ is contained in $\mathbf{t}_{L,j,M-1-K}$.

By adding vertical floors to the first and last floors, we can align the nontrivial dominoes in $\mathbf{t}$ and $\mathbf{t}_{L,j,M-1-K}$, so that both tilings now have the same height and contain the same nontrivial dominoes. Consequently, they define two tilings of the same planar non simply connected region. The choice of j implies that these two tilings have the same flux. Thus, it follows that $\mathbf{t} \sim \mathbf{t}_{L,j,M-1-K}$. ■

Lemmas 5.2 and 5.3 imply that $G^+_{\mathcal{D}_L}$ is generated by the tilings $\mathbf{t}_{L,j}$. We now reduce this family to two generators. Notice that the first two tilings in Figure 5.4 are inverses of each other, as are the last two tilings. The remaining tilings are equivalent to the vertical tiling, as four flips transform each of them into a tiling that contains no nontrivial dominoes. Thus, $G^+_{\mathcal{D}_L}$ is generated by the first and last tilings $\mathbf{t}_L = \mathbf{t}_{L,1}$ and $\tilde{\mathbf{t}}_L = \mathbf{t}_{L,8}$. Since $\mathbf{t}_L$ and $\tilde{\mathbf{t}}_L$ are composed of vertical dominoes in $[L, 2L] \times [0,1] \times [0,6]$ and $[0, L] \times [0,1] \times [0,6]$, respectively, and since vertical floors can be moved via flips, we have that $\mathbf{t}_L$ and $\tilde{\mathbf{t}}_L$ commute: $\mathbf{t}_L * \tilde{\mathbf{t}}_L * \mathbf{t}_L^{-1} * \tilde{\mathbf{t}}_L^{-1} \approx \mathbf{t}_{\mathrm{vert}}$.

Proof of Proposition 5.1. Given a tiling of $\mathcal{D}_L \times [0, 2N]$ we obtain another tiling by reflecting on the plane $x + y = 2L - 1$ the dominoes contained in $(s_L \cup ([2L-2, 2L] \times [0,1])) \times [0, 2N]$; as with the two tilings in Figure 5.2. This construction defines an automorphism $\psi\colon G^+_{\mathcal{D}_L} \to G^+_{\mathcal{D}_L}$. Then, the map $\phi\colon G^+_{\mathcal{D}_L} \to \mathbb{Z}\oplus\mathbb{Z}$ that takes a tiling $\mathbf{t}$ to $(\mathrm{Tw}(\mathbf{t}), \mathrm{Tw}\circ\psi(\mathbf{t}))$ is a homomorphism. We have that $\phi(\mathbf{t}_L) = (-1, 1)$ and $\phi(\tilde{\mathbf{t}}_L) = (1,1)$. Thus, the image of ϕ is isomorphic to $\mathbb{Z} \oplus \mathbb{Z}$. Moreover, since $\mathbf{t}_L$ and $\tilde{\mathbf{t}}_L$ commute, ϕ is injective. ■

Remark 5.4. In cases where $G^+_{\mathcal{D}}$ is isomorphic to $\mathbb{Z}^2$, we can obtain a bound on the size of the flip connected components of $\mathcal{T}(\mathcal{R}_N)$, as with Theorem 1.1. Specifically, the size of the components is $O(N^{-1}|\mathcal{T}(\mathcal{R}_N)|)$. Indeed, by following the proof of Theorem 1.1, it suffices to show that there exists a constant $C > 0$ such that $\mathbb{P}(y_0 X_1 y_1 \dots X_t y_t = e) \le C t^{-1}$ for all $t \ge 0$, where $(X_t)_{t\ge1}$ denotes a lazy random walk on $\mathbb{Z}^2$ and $(y_t)_{t\ge0}$ is a sequence of elements in $\mathbb{Z}^2$. Since $\mathbb{Z}^2$ is abelian, we have $\mathbb{P}(y_0 X_1 y_1 \dots X_t y_t = e) = \mathbb{P}(X_1 X_2 \dots X_t = (y_0 y_1 \dots y_t)^{-1})$, and the desired bound then follows from a local central limit theorem. We conjecture that the size of the largest flip connected component is in fact $\Theta(N^{-1}|\mathcal{T}(\mathcal{R}_N)|)$. ◇

5.2 Strongly irregular disks

This section presents a study of strongly irregular disks. Preliminary work from the author's master's thesis [16] established Theorem 5.5, which demonstrates the strong irregularity of the disks depicted in Figure 5.5. Theorem 1.5 generalizes a result from [16], while Theorem 1.4 presents a new class of strongly irregular disks. The proofs of these theorems are similar and are included to ensure the completeness of the text.

Theorem 5.5. *Consider a balanced quadriculated disk $\mathcal{D}$. Suppose there is a 2×2 square $s \subset \mathcal{D}$ such that $\mathcal{D} \smallsetminus s$ is the union of two disjoint disks $\mathcal{D}_1$ and $\mathcal{D}_2$ with $|\mathcal{D}_1| = |\mathcal{D}_2|$. Suppose s contains dominoes d_1 adjacent to $\mathcal{D}_1$ and d_2 adjacent to $\mathcal{D}_2$ such that $\mathcal{D} \smallsetminus d_1$ and $\mathcal{D} \smallsetminus d_2$ are not connected. Then, $\mathcal{D}$ is strongly irregular.*

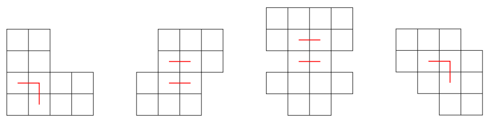

Figure 5.5: Examples of strongly irregular disks; dominoes d_1 and d_2 as in Theorem 5.5 are marked by a red line segment.

The proofs of strong irregularity rely on constructing surjective homomorphisms to the free group F_2. To achieve this, we adopt a general strategy. Given a disk $\mathcal{D}$, we first construct a map Φ that takes oriented edges (floors with parity) in $\mathcal{C}_{\mathcal{D}}^{+}$ to F_2. In particular, Φ defines a homomorphism from the free group on oriented edges to F_2. Secondly, we verify that Φ maps the boundary of any 2-cell to the identity. As a consequence, we obtain a homomorphism $\phi\colon G_{\mathcal{D}}^{+} \to F_2$ by taking the quotient of the free group on oriented edges by the relations defining $G_{\mathcal{D}}^{+}$. In order to fix the ideas, consider Example 5.6, which exhibits the only disk that we know of whose strong irregularity does not follow from our results.

Example 5.6. Let $\mathcal{D}$ be the disk formed by the union of the rectangle $[0,4] \times [0,1]$ and the two unit squares $[1,2] \times [-1,0]$ and $[2,3] \times [1,2]$. We construct a surjective homomorphism $\phi\colon G_{\mathcal{D}}^{+} \to F_2$.

Let $d = [1,3] \times [0,1]$ be a domino and let $p_0 = [0,1]^2 \cup ([2,3] \times [1,2])$ and $p_1 = ([1,2] \times [-1,0]) \cup ([3,4] \times [0,1])$ be plugs. Then, $f = (p_0, d, p_1)$ defines an oriented edge of the complex $\mathcal{C}_{\mathcal{D}}$. We then obtain four oriented edges in $\mathcal{C}_{\mathcal{D}}^{+}$, i.e., floors with parity: $\mathbf{f_0} = (f, 0)$, $\mathbf{f_1} = (f^{-1}, 0)$, $\mathbf{f_0}^{-1} = (f^{-1}, 1)$ and $\mathbf{f_1}^{-1} = (f, 1)$.

We now define Φ for oriented edges in $\mathcal{C}_{\mathcal{D}}^{+}$. Set $\Phi(\mathbf{f_0}) = a$, $\Phi(\mathbf{f_1}) = b$, $\Phi(\mathbf{f_0}^{-1}) = a^{-1}$ and $\Phi(\mathbf{f_1}^{-1}) = b^{-1}$; all other edges are mapped to the identity.

The map Φ takes the boundary of any 2-cell in $\mathcal{C}_{\mathcal{D}}^{+}$ to the identity, as $\mathbf{f_i}$ do not permit horizontal flips and the possible vertical flip is obtained by moving consecutively along $\mathbf{f_i}$ and $\mathbf{f_i}^{-1}$. Thus, Φ extends to a homomorphism $\phi\colon G_{\mathcal{D}}^{+} \to F_2$. Notice that $\phi(\mathbf{t}) = a$ and $\phi(\tilde{\mathbf{t}}) = b$ for the tilings $\mathbf{t}$ and $\tilde{\mathbf{t}}$ shown in Figure 5.6, so that ϕ is surjective. By following the ideas of Section 5.1, one can further show that $\mathbf{t}$ and $\tilde{\mathbf{t}}$ generate $G_{\mathcal{D}}^{+}$, implying that ϕ is in fact an isomorphism. ◇

Figure 5.6: Tilings $\mathbf{t}$ and $\tilde{\mathbf{t}}$ of $\mathcal{D} \times [0, 6]$. The map Φ takes the second floor of $\mathbf{t}$ and $\tilde{\mathbf{t}}$ to a and b, respectively.

Proof of Theorem 1.4. We first consider the case in which $\mathcal{D} \smallsetminus s$ has exactly three connected components $\mathcal{D}_1$, $\mathcal{D}_2$ and $\mathcal{D}_3$. Suppose that $|\mathcal{D}_1| \leq |\mathcal{D}_2| \leq |\mathcal{D}_3|$. By hypothesis, $|\mathcal{D}_1 \cup \mathcal{D}_2| \geq 3$. For $i \in \{1, 2, 3\}$, let $s_i \subset \mathcal{D}_i$ be a unit square adjacent to s and let $d_i = s \cup s_i$ be a domino.

We define two classes of floors $\mathcal{F}_0$ and $\mathcal{F}_1$. A floor (p_0, f^*, p_1) belongs to $\mathcal{F}_0$ if and only if:

1. f^* contains the domino d_1.
2. p_0 marks all white squares in $\mathcal{D}_1 \smallsetminus s_1$ and all black squares in $\mathcal{D}_2$.
3. p_1 marks all black squares in $\mathcal{D}_1 \smallsetminus s_1$ and all white squares in $\mathcal{D}_2$.

A floor belongs to $\mathcal{F}_1$ if and only if its inverse belongs to $\mathcal{F}_0$; Figure 5.7 shows an example of a disk and its classes $\mathcal{F}_0$ and $\mathcal{F}_1$. This defines four classes of floors with parity: $\mathbf{f_0} = (\mathcal{F}_0, 0)$, $\mathbf{f_1} = (\mathcal{F}_1, 0)$, $\mathbf{f_0}^{-1} = (\mathcal{F}_1, 1)$ and $\mathbf{f_1}^{-1} = (\mathcal{F}_0, 1)$.

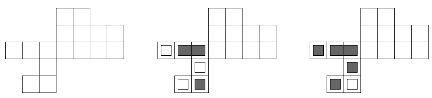

Figure 5.7: A disk and its two classes of floors $\mathcal{F}_0$ and $\mathcal{F}_1$.

We initially define a map Φ for oriented edges in $\mathcal{C}_{\mathcal{D}}^{+}$. If a floor with parity $\mathbf{f}$ is not contained in the classes defined above, let $\Phi(\mathbf{f}) = e$. Otherwise, set $\Phi(\mathbf{f_0}) = a$, $\Phi(\mathbf{f_1}) = b$, $\Phi(\mathbf{f_0}^{-1}) = a^{-1}$ and $\Phi(\mathbf{f_1}^{-1}) = b^{-1}$.

Consider two adjacent floors with parity in $\mathcal{C}_{\mathcal{D}}^{+}$ (i.e., an oriented path of length two) whose reduced floors contain the domino d_1. We have only two possibilities. First, both floors are neither in $\mathcal{F}_0$ nor in $\mathcal{F}_1$. Second, either the first floor is in $\mathcal{F}_0$ and the second floor is in $\mathcal{F}_1$ or vice-versa. Since adjacent edges have opposite parity, in any case we conclude that Φ maps this path of length two to the identity. With this observation in mind, it is straightforward to check that Φ maps the boundary of any 2-cell to the identity. Therefore, Φ extends to a homomorphism $\phi\colon G_{\mathcal{D}}^{+} \to F_2$.

We now prove the surjectivity of ϕ. Suppose, without loss of generality, that s is a white unit square. Let $\tilde{s_3} \subset \mathcal{D}_3$ and $\tilde{s_2} \subset \mathcal{D}_2$ be unit squares adjacent to s_3 and s_2, respectively. Consider a floor $f = (p_0, d_1, p_1)$ in $\mathcal{F}_0$ such that $p_1 = p_0^{-1} \smallsetminus d_1$. We may assume that $s_3 \not\subset p_0$ and $\tilde{s_3} \subset p_0$. Since s disconnects $\mathcal{D}$, for any spanning tree of $\mathcal{D}$, we have that $\tilde{s_2}$ and s_3 are the two nonadjacent unit squares of opposite colors in p_1 at minimal distance. Then, by construction, the floors of $\mathbf{t}_{p_1}$ (recall Remark 2.2) are contained neither in $\mathcal{F}_0$ nor in $\mathcal{F}_1$. Let $p = (p_1 \smallsetminus s_3) \cup s_1$ be a plug and $g = (p, d_3, p_0)$ be a floor. Analogously, the floors of $\mathbf{t}_p$ are contained neither in $\mathcal{F}_0$ nor in $\mathcal{F}_1$. Thus, $\mathbf{t} = \mathbf{t}_p^{-1} * g * f * \mathbf{t}_{p_1}$ is a tiling such that $\phi(\mathbf{t}) = a$. Similarly, consider the plug $\tilde{p} = (p_0 \smallsetminus s_2) \cup s_1$ and the floor $\tilde{g} = (\tilde{p}, d_2, p_1)$. Then, the tiling $\tilde{\mathbf{t}} = \mathbf{t}_{\tilde{p}}^{-1} * \tilde{g} * f^{-1} * \mathbf{t}_{p_0}$ is such that $\phi(\tilde{\mathbf{t}}) = b$.

Now, consider the case in which there exists a fourth connected component $\mathcal{D}_4$. By possibly relabeling the components, assume that $|\mathcal{D}_1| \leq |\mathcal{D}_2| \leq |\mathcal{D}_3| \leq |\mathcal{D}_4|$. Proceed as in the previous case if $|\mathcal{D}_3| > 1$: define two classes containing floors (p_0, f^*, p_1) such that $d_1 \subset f^*$ and the plugs p_0 and p_1 mark alternately the unit squares in $\mathcal{D}_1 \cup \mathcal{D}_2 \cup \mathcal{D}_3$.

Suppose that $|\mathcal{D}_1| = |\mathcal{D}_2| = |\mathcal{D}_3| = 1$. We define two classes of floors $\mathcal{F}_0$ and $\mathcal{F}_1$. A floor (p_0, f^*, p_1) belongs to $\mathcal{F}_0$ if and only if $d_1 \subseteq f^*$, $s_2 \subset p_0$ and $s_3 \subset p_1$. A floor belongs to $\mathcal{F}_1$ if and only if its inverse belongs to $\mathcal{F}_0$; see Figure 5.8. As in the previous case, we have four classes with parity and a homomorphism $\phi\colon G_{\mathcal{D}}^{+} \to F_2$.

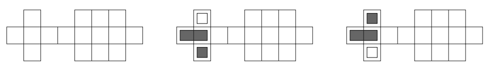

Figure 5.8: A disk and its two classes of floors $\mathcal{F}_0$ and $\mathcal{F}_1$.

Let $f = (p_0, d_1, p_1)$ be a floor in $\mathcal{F}_0$ such that $p_1 = p_0^{-1} \smallsetminus d_1$. Let $p = (p_1 \smallsetminus s_3) \cup s_1$ be a plug and $g = (p, d_3, p_0)$ be a floor. Then, by construction, the floors of $\mathbf{t}_{p_1}$ and $\mathbf{t}_p$ are contained neither in $\mathcal{F}_0$ nor in $\mathcal{F}_1$. Thus, we have $\phi(\mathbf{t}) = a$ for $\mathbf{t} = \mathbf{t}_p^{-1} * g * f * \mathbf{t}_{p_1}$. Similarly, we obtain $\tilde{\mathbf{t}}$ such that $\phi(\tilde{\mathbf{t}}) = b$. ■

Proof of Theorem 1.5. The proof consists of two cases. We define, in both cases, two classes of floors $\mathcal{F}_0$ and $\mathcal{F}_1$. The class $\mathcal{F}_1$ contains a floor if and only if its inverse belongs to $\mathcal{F}_0$, so that it suffices to define $\mathcal{F}_0$.

First consider the case in which there exists only one 2×2 square containing d; denote this square by s. Let $\mathcal{D}_0$ be the connected component of $\mathcal{D} \smallsetminus d$ that intersects s. In this case, a floor (p_0, f^*, p_1) belongs to $\mathcal{F}_0$ if and only if $d \subset f^*$ and p_0 (resp. p_1) marks all black (resp. white) squares in $\mathcal{D}_0$; as in Figure 5.9.

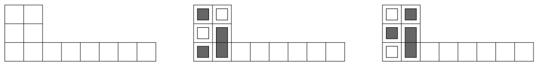

Figure 5.9: A disk and its two classes of floors $\mathcal{F}_0$ and $\mathcal{F}_1$.

The second case is based on the existence of two distinct 2×2 squares $s_1, s_2 \subset \mathcal{D}$ such that $d \subset s_1$ and $d \subset s_2$. Let $\mathcal{D}_1$ (resp. $\mathcal{D}_2$) be the connected component of $\mathcal{D} \smallsetminus s$ that intersects s_1 (resp. s_2). Suppose that $|\mathcal{D}_1| \leq |\mathcal{D}_2|$. In this case, a floor (p_0, f^*, p_1) belongs to $\mathcal{F}_0$ if and only if:

1. f^* contains the domino d.

2. p_0 marks all black squares in $\mathcal{D}_1$ and all white squares in $\mathcal{D}_2$.

3. p_1 marks all white squares in $\mathcal{D}_1$ and all black squares in $\mathcal{D}_2$.

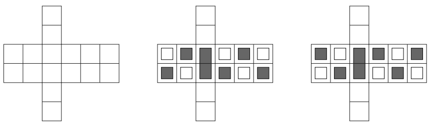

Figure 5.10: A disk and its two classes of floors $\mathcal{F}_0$ and $\mathcal{F}_1$.

Notice that the classes of floors are nonempty. Indeed, by hypothesis, in the first case $|\mathcal{D} \smallsetminus d| - |\mathcal{D}_0| \geq |\mathcal{D}_0|$ and in the second case $|\mathcal{D} \smallsetminus d| - |\mathcal{D}_1| - |\mathcal{D}_2| \geq |\mathcal{D}_2| - |\mathcal{D}_1|$. Therefore, since $\mathcal{D}$ is balanced, in both cases there exist plugs satisfying the required properties.

As in the proof of Theorem 1.4, we have four floors with parity which define Φ for oriented edges in $\mathcal{C}^+_{\mathcal{D}}$. By construction, in a floor (p_0, f^*, p_1) of class either $\mathcal{F}_0$ or $\mathcal{F}_1$, each connected component of $\mathcal{D} \smallsetminus d$ that intersects a 2×2 square which contains d is marked alternately by p_0 and p_1. Then, again as in the proof of Theorem 1.4, it is not difficult to check that Φ takes the boundary of any 2-cell to the identity. Thus, Φ extends to a homomorphism $\phi\colon G^+_{\mathcal{D}} \to F_2$.

We are left to show that ϕ is surjective. Consider a floor $f = (p_0, d_1, p_1)$ in $\mathcal{F}_0$ such that $p_1 = p_0^{-1} \smallsetminus d_1$. Notice that, since d is contained in a 2×2 square, there exists a spanning tree of $\mathcal{D}$ whose set of edges does not contain d. Then, by definition, the tilings $\mathbf{t} = \mathbf{t}_{p_0}^{-1} * f * (p_1, \emptyset, p_1^{-1}) * \mathbf{t}_{p_1^{-1}}$ and $\tilde{\mathbf{t}} = \mathbf{t}_{p_1}^{-1} * f^{-1} * (p_0, \emptyset, p_0^{-1}) * \mathbf{t}_{p_0^{-1}}$ are such that $\phi(\mathbf{t}) = a$ and $\phi(\tilde{\mathbf{t}}) = b$. ∎

6
Regular disks

This chapter is dedicated to the proofs of Theorems 1.6 and 1.7.

6.1
Hamiltonian disks

In this section, we present the advantages of using hamiltonian disks and establish two technical lemmas. Although these results may initially seem disconnected, their importance will become evident in the next section.

Lemma 6.1. *Let $\mathcal{D}$ be a disk with a hamiltonian cycle $\gamma = (s_1, s_2, \ldots, s_{|\mathcal{D}|})$. Consider two dominoes $d = s_k \cup s_l$ and $\tilde{d} = s_i \cup s_j$ that do not respect γ. Suppose that $l - k \geq 5$. If $i < k < j < l$ (resp. $k < j < l < i$) then* $\max\{k-i, l-j\} \geq 3$ *(resp.* $\max\{j-k, i-l\} \geq 3$*).*

Proof. Let $i < k < j < l$, the other case is similar. Suppose, for a contradiction, that $k - i < 3$ and $l - j < 3$. Since $|\mathcal{D}_{\tilde{d},0}|$ is even and positive, $j - i$ is an odd number; analogously, $l - k$ is odd. Thus, either $k - i = 1 = l - j$ or $k - i = 2 = l - j$. In the first case, (s_i, s_k, s_l, s_j) defines a cycle of length four and therefore corresponds to a 2×2 square in $\mathcal{D}$. In the second case, $(s_k, s_{i+1}, s_i, s_j, s_{j+1}, s_l)$ defines a cycle of length six and therefore corresponds to a 3×2 rectangle in $\mathcal{D}$. Then, γ essentially follows one of the four patterns shown in Figure 6.1.

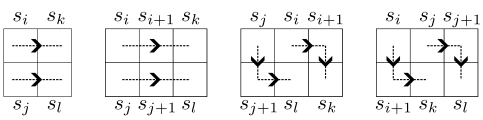

Figure 6.1: Four possible configurations of γ.

However, in any of these four possibilities we have a contradiction with the fact that s_1 and $s_{|\mathcal{D}|}$ are adjacent. Indeed, in the first three cases the cycle $(s_i, \ldots, s_j)$ defines two regions in $\mathcal{D}$ that separate s_1 and $s_{|\mathcal{D}|}$. The fourth case follows by the same argument once we observe that s_j and s_k are not adjacent, as $l - k \geq 5$. ■

Let $\mathcal{D}$ be a disk with a hamiltonian cycle $\gamma = (s_1, s_2, \ldots, s_{|\mathcal{D}|})$. By relabeling the unit squares, we can choose any unit square in $\mathcal{D}$ to be the initial square of γ. We will need that a hamiltonian cycle starts at a corner, i.e., a unit square that is adjacent to only other two unit squares. Let s_{SW} be the southwesternmost unit square in $\mathcal{D}$, i.e.,

$$s_{SW} = [a, a+1] \times [b, b+1], \text{ where}$$
$$b = \min\{y \in \mathbb{Z} : (x, y) \in \mathcal{D} \text{ for some } x \in \mathbb{Z}\} \text{ and } a = \min\{x \in \mathbb{Z} : (x, b) \in \mathcal{D}\}$$

Notice that s_{SW} is a corner of $\mathcal{D}$. Moreover, if s is a unit square adjacent to s_{SW} then $\mathcal{D} \smallsetminus (s \cup s_{SW})$ is a path-hamiltonian disk.

A hamiltonian cycle corresponds to a simple closed curve that passes through the center of every unit square in $\mathcal{D}$, as in Figure 2.3. Thus, γ divides $\mathcal{D}$ into two connected components, one of the components is contractible and the other is non-contractible. The contractible connected component is called the *interior* of γ, the non-contractible component is called the *exterior* of γ. We say that a domino $d = s_k \cup s_l$ is contained in the interior (resp. exterior) of γ if the line segment between the centers of s_k and s_l intersects the interior (resp. exterior) of γ; for instance, see Figure 6.2. Notice that, except by $s_1 \cup s_{|\mathcal{D}|}$, every domino that does not respect γ is contained in either the interior or the exterior of γ. This fact help us to prove Lemma 6.2 below.

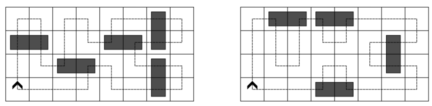

Figure 6.2: The first (resp. second) example shows dominoes contained in the interior (resp. exterior) of a cycle γ.

Lemma 6.2. *Let $\mathcal{D}$ be a disk with a hamiltonian cycle $\gamma = (s_1, s_2, \ldots, s_{|\mathcal{D}|})$ starting at $s_1 = s_{SW}$. Consider two distinct dominoes $d, \tilde{d} \in \mathcal{D}_\gamma$. There exist dominoes $d_1, d_2, \ldots, d_n$ with $d_1 = \tilde{d}$ and $d_n = d$ such that, for each $i \in \{1, 2, \ldots, n-1\}$, one of the following holds:*

1. *d_{i+1} is the union of a unit square in $\mathcal{D}_{d_i,0}$ and a unit square in $\mathcal{D}_{d_i,\pm 1}$.*

2. *$d_{i+1} \subset \mathcal{D}_{d_i,0}$ and $\mathcal{D}_{d_i,0} \smallsetminus \mathcal{D}_{d_{i+1},0}$ is a disk.*

3. *$d_{i+1} \subset \mathcal{D}_{d_i,\pm 1}$ and $\mathcal{D}_{d_i,\pm 1} \smallsetminus \mathcal{D}_{d_{i+1},\pm 1}$ is a disk.*

Proof. Throughout the proof, we say that two dominoes $\bar{d}_1, \bar{d}_2 \in \mathcal{D}_\gamma$ form a good pair if the result holds for $d = \bar{d}_1$ and $\tilde{d} = \bar{d}_2$. We show that any two dominoes that do not respect γ form a good pair. The proof is by induction on $|\mathcal{D}|$, with the base case being when $|\mathcal{D}| = 4$. In this case, $\mathcal{D}$ is a 2×2 square and the result follows vacuously.

In order to prove the induction step, we first consider the case that there exists a domino $\hat{d}$ that disconnects $\mathcal{D}$; clearly, $\hat{d} \in \mathcal{D}_\gamma$. By possibly changing the orientation of γ ($s_1 = s_{SW}$ still holds) we may assume that $\hat{d}$ and $s_1 \cup s_{|\mathcal{D}|}$ are disjoint. Notice that $\hat{d}$ defines two other disks $\mathcal{D}_1 = \mathcal{D} \setminus \mathcal{D}_{\hat{d},0}$ and $\mathcal{D}_2 = \mathcal{D} \setminus \mathcal{D}_{\hat{d},\pm 1}$ such that $\mathcal{D} = \mathcal{D}_1 \cup \mathcal{D}_2$ and $\mathcal{D}_1 \cap \mathcal{D}_2 = \hat{d}$; for instance, see Figure 6.3. The cycle γ induces hamiltonian cycles γ_1 in $\mathcal{D}_1$ and γ_2 in $\mathcal{D}_2$; the union of the initial and final squares of γ_1 and γ_2 constitute $s_1 \cup s_{|\mathcal{D}|}$ and $\hat{d}$, respectively. Hence, by the induction hypothesis, it suffices to show that $s_1 \cup s_{|\mathcal{D}|}$ and $\hat{d}$ form a good pair. On the other hand, since $\hat{d}$ is disjoint from $s_1 \cup s_{|\mathcal{D}|}$ and $s_1 = s_{SW}$, we have that $\mathcal{D}_{s_1 \cup s_{|\mathcal{D}|},0} \setminus \mathcal{D}_{\hat{d},0} = \mathcal{D}_1 \setminus (s_1 \cup s_{|\mathcal{D}|})$ is a disk.

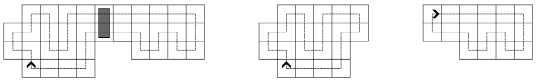

Figure 6.3: A hamiltonian disk $\mathcal{D}$ with a domino $\hat{d}$ that disconnects $\mathcal{D}$ and the induced hamiltonian disks $\mathcal{D} \setminus \mathcal{D}_{\hat{d},0}$ and $\mathcal{D} \setminus \mathcal{D}_{\hat{d},\pm 1}$.

Now, suppose there exists no domino that disconnects $\mathcal{D}$. Therefore, every domino $\hat{d} \in \mathcal{D}_\gamma \setminus \{s_1 \cup s_{|\mathcal{D}|}\}$ forms a good pair with a domino $\bar{d}$ composed of a unit square in $\mathcal{D}_{\hat{d},0}$ and a unit square in $\mathcal{D}_{\hat{d},\pm 1}$. Notice that if $\hat{d}$ is contained in the interior of γ then $\bar{d}$ is contained in the exterior of γ, and vice versa. Moreover, by possibly altering the orientation of γ, as in the previous paragraph, it is not difficult to see that the 2×2 square that contains $s_1 = s_{SW}$ also contains a domino that forms a good pair with $s_1 \cup s_{|\mathcal{D}|}$. Thus, the result follows once we prove that any two dominoes in the exterior of γ form a good pair.

Let $\partial\mathcal{D} \subset \mathcal{D}$ be the union of the unit squares not contained in the topological interior of $\mathcal{D}$. Let $d^1, d^2, \ldots, d^j$ be the dominoes in $\partial\mathcal{D}$ that are distinct from $s_1 \cup s_{|\mathcal{D}|}$ and do not respect γ; for an example, see Figure 6.4. Clearly, these dominoes are contained in the exterior of γ. Notice that every domino in the exterior of γ is contained in the pairwise disjoint union $\bigcup_{m=1}^{j} \mathcal{D}_{d^m,0} \cup d^m$. Since γ induces a hamiltonian cycle in $\mathcal{D}_{d^m,0} \cup d^m$, it follows from the the induction hypothesis that d^m form a good pair with every domino in $\mathcal{D}_{d^m,0}$ that does not respect γ. We are left to show that d^r and d^s form a good pair for any $r, s \in \{1, 2, \ldots, j\}$.

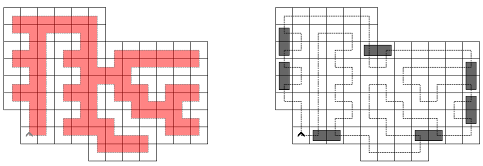

Figure 6.4: A disk $\mathcal{D}$ with the interior of a hamiltonian cycle shown in red, and the dominoes in $\partial\mathcal{D}$ that are distinct from $s_1 \cup s_{|\mathcal{D}|}$ and do not respect γ.

The fact that there is no domino that disconnects $\mathcal{D}$ implies that every non-corner unit square in $\partial\mathcal{D}$ is adjacent to a unit square not in $\partial\mathcal{D}$, so that

$\mathcal{D} \setminus \partial\mathcal{D}$ is connected. Then, by possibly relabeling the dominoes $d^1, d^2, \ldots, d^j$, we may assume that for each m we have a unit square in $\mathcal{D}_{d^{m+1},0}$ adjacent to a unit square in $\mathcal{D}_{d^m,0} \subset \mathcal{D}_{d^{m+1},\pm 1}$. Thus, d^m and d^{m+1} form a good pair. ∎

6.2 Proof of Theorems 1.6 and 1.7

The strategy of our proof is to demonstrate that a disk $\mathcal{D}$ satisfying either Theorem 1.6 or Theorems 1.7 has a cyclic even domino group. We reduce the family of generators of $G^+_{\mathcal{D}}$, as defined in Section 2.1, to a single element. To achieve this, we demonstrate a series of results that reveal additional properties of the flux for hamiltonian disks.

The following two lemmas show that for a given domino $d \subset \mathcal{D}$, instead of considering all possible triples $\operatorname{flux}(d, \cdot)$, it is sufficient to examine all possible nonzero integers $\operatorname{flux}_0(d, \cdot)$.

Lemma 6.3. *Let $\mathcal{D}$ be a disk with a hamiltonian cycle $\gamma = (s_1, s_2, \ldots, s_{|\mathcal{D}|})$ starting at $s_1 = s_{SW}$. Consider a domino $d \in \mathcal{D}_\gamma$ with a compatible plug $p \in \mathcal{P}_d$. If* $\operatorname{flux}_0(d, p) = 0$ *then* $\mathbf{t}_{d,p} \sim \mathbf{t}_{vert}$.

Proof. Suppose that $p \cap \mathcal{D}_{d,0} = \varnothing$; otherwise, for the plug $\tilde{p} = p \cap \mathcal{D}_{d,\pm 1}$ we have $\operatorname{flux}(d, p) = \operatorname{flux}(d, \tilde{p})$ and therefore, by Fact 2.5, $\mathbf{t}_{d,p} \sim \mathbf{t}_{d,\tilde{p}}$. The tiling $\mathbf{t}_{d,p}$ then covers the region $\mathcal{D}_{d,0} \times [|p|, |p| + 2]$ solely with vertical dominoes.

Let $\mathbf{t}_1$ be the tiling obtained from $\mathbf{t}_{d,p}$ by performing vertical flips along $\gamma_{d,0}$, so that the restriction of $\mathbf{t}_1$ to $(\mathcal{D}_{d,0} \cup d) \times [|p|, |p| + 1]$ is occupied only by horizontal dominoes. Notice that $\mathcal{D}_{d,0} \cup d$ is a disk, as it is defined by the cycle $(s_k, s_{k+1}, \ldots, s_l)$ and neither s_1 nor $s_{|\mathcal{D}|}$ is contained in the interior of $\mathcal{D}$. Since the space of tilings of a disk is connected under flips, there exists a sequence of horizontal flips that takes $\mathbf{t}_1$ to the tiling $\mathbf{t}_2$ whose restriction to $(\mathcal{D}_{d,0} \cup d) \times [|p|, |p| + 1]$ corresponds to the tiling induced by $(s_k, s_{k+1}, \ldots, s_l)$. Thus, $\mathbf{t}_{d,p} \approx \mathbf{t}_1 \approx \mathbf{t}_2$ and every domino in $\mathbf{t}_2$ respects γ. It follows from Fact 2.1 that $\mathbf{t}_2 \sim \mathbf{t}_{\text{vert}}$. ∎

Lemma 6.4. *Let $\mathcal{D}$ be a disk with a hamiltonian cycle $\gamma = (s_1, s_2, \ldots, s_{|\mathcal{D}|})$ starting at $s_1 = s_{SW}$. Consider a domino $d \in \mathcal{D}_\gamma$ and two plugs $p_1, p_2 \in \mathcal{P}_d$. If* $\operatorname{flux}_0(d, p_1) = \operatorname{flux}_0(d, p_2)$ *then* $\mathbf{t}_{d,p_1} \sim \mathbf{t}_{d,p_2}$.

Proof. Throughout this proof, in addition to γ, we also work with another hamiltonian cycle $\tilde{\gamma}$. To avoid confusion, we distinguish the flux between a domino and plug with respect to each cycle. Specifically, we denote the flux with respect to $\tilde{\gamma}$ and γ by $\operatorname{flux}(\cdot, \cdot; \tilde{\gamma})$ and $\operatorname{flux}(\cdot, \cdot; \gamma)$, respectively. Similarly, we refer to the three subregions of $\mathcal{D}$ determined by a domino that does not respect a given cycle.

Suppose that $d = s_k \cup s_l$ with $k < l$, so that $l - k \geq 3$. Consider the hamiltonian cycle $\tilde{\gamma} = (s_{k+1}, s_k, \ldots, s_1, s_{|\mathcal{D}|}, s_{|\mathcal{D}|-1}, \ldots, s_{k+2})$ obtained by changing the initial square of γ; for instance, see Figure 6.5.

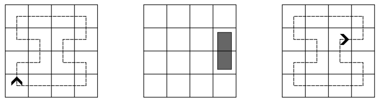

Figure 6.5: A disk with a hamiltonian cycle γ, a domino d and the cycle $\tilde{\gamma}$ obtained from γ.

We claim that if p is a plug compatible with d then $\mathbf{t}_{d,p;\gamma} \sim \mathbf{t}_{d,p;\tilde{\gamma}}$. By construction, a domino in $\mathbf{t}_{d,p;\tilde{\gamma}}$ which does not respect γ and does not project on d is of the form $d_1 \times [N-1, N]$ with $d_1 = s_1 \cup s_{|\mathcal{D}|}$. Then, from the facts in Section 2.1, $\mathbf{t}_{d,p;\tilde{\gamma}}$ is $\sim$-equivalent to a concatenation of $\mathbf{t}_{d,p;\gamma}$ and possibly tilings $\mathbf{t}_{d_1,\hat{p};\gamma}$. However, we have $\operatorname{flux}(d_1, \hat{p}; \gamma) = (0, 0, 0)$ for any plug $\hat{p} \in \mathcal{P}_{d_1}$. Thus, by Lemma 6.3, $\mathbf{t}_{d_1,\hat{p};\gamma} \sim \mathbf{t}_{\text{vert}}$. Therefore, $\mathbf{t}_{d,p;\gamma} \sim \mathbf{t}_{d,p;\tilde{\gamma}}$.

Let $\hat{p_1}$ be the plug formed by the union of $p_2 \cap \mathcal{D}_{d,0;\gamma}$ and $p_1 \cap \mathcal{D}_{d,\pm 1;\gamma}$. Notice that $\operatorname{flux}(d, \hat{p_1}; \gamma) = \operatorname{flux}(d, p_1; \gamma)$ and $\operatorname{flux}(d, \hat{p_1}; \tilde{\gamma}) = \operatorname{flux}(d, p_2; \tilde{\gamma})$. Thus, by the previous claim and Fact 2.5, $\mathbf{t}_{d,p_1;\gamma} \sim \mathbf{t}_{d,\hat{p_1};\gamma} \sim \mathbf{t}_{d,\hat{p_1};\tilde{\gamma}} \sim \mathbf{t}_{d,p_2;\tilde{\gamma}} \sim \mathbf{t}_{d,p_2;\gamma}$. ∎

We now consider tilings $\mathbf{t}_{d,p}$ with large flux, those where $|\operatorname{flux}_0(d,p)| \geq 2$. In Lemma 6.5, we show that in certain cases, such tilings can be decomposed into a concatenation of tilings with smaller flux. As a consequence, it follows that the even domino group of a bottleneck-free disk is generated by tilings with $|\operatorname{flux}_0(\cdot,\cdot)| = 1$.

Lemma 6.5. *Let $\mathcal{D}$ be a disk with a hamiltonian cycle $\gamma = (s_1, s_2, \ldots, s_{|\mathcal{D}|})$ starting at $s_1 = s_{SW}$. Consider a domino $d \in \mathcal{D}_\gamma$ such that $\mathcal{D} \smallsetminus d$ is connected. Let p be a plug compatible with d such that $|\operatorname{flux}_0(d,p)| \geq 2$. Then, there exist plugs $p_0, p_1, p_2 \in \mathcal{P}$ and a domino $\tilde{d} \in \mathcal{D}_\gamma$ that does not disconnect $\mathcal{D}$ such that:*

1. $\mathbf{t}_{d,p} \sim \mathbf{t}_{\tilde{d},p_1}^{\epsilon_1} * \mathbf{t}_{d,p_0} * \mathbf{t}_{\tilde{d},p_2}^{\epsilon_2}$ *for some* $\epsilon_1, \epsilon_2 \in \{-1, 1\}$.
2. $\max\{|\operatorname{flux}_0(\tilde{d}, p_1)|, |\operatorname{flux}_0(d, p_0)|, |\operatorname{flux}_0(\tilde{d}, p_2)|\} < |\operatorname{flux}_0(d,p)|$.

Proof. Since $\mathcal{D} \smallsetminus d$ is connected, there exists a domino $\tilde{d} = s_i \cup s_j$ such that $s_i \in \mathcal{D}_{d,\pm 1}$ and $s_j \in \mathcal{D}_{d,0}$. We have $s_i \neq s_1$; otherwise the fact that s_1 is a corner implies that $s_j = s_{\mathcal{D}}$, which is not an element of $\mathcal{D}_{d,0}$. Notice that $\mathcal{D} \smallsetminus \tilde{d}$ is also connected, as d is formed by unit squares contained in $\mathcal{D}_{\tilde{d},0}$ and $\mathcal{D}_{\tilde{d},\pm 1}$. Suppose that $s_i \in \mathcal{D}_{d,-1}$, the case $s_i \in \mathcal{D}_{d,+1}$ is analogous.

Consider first the scenario where $\operatorname{color}(s_j) = \operatorname{sign}(\operatorname{flux}_0(d,p))$. Suppose $d = s_k \cup s_l$, with $k < l$. Since $|\operatorname{flux}_0(d,p)| \geq 2$, we have $l - k \geq 5$. By Lemma 6.1 it follows that $\max\{k - i, l - j\} \geq 3$. Consequently, by Lemma 6.4, we may assume, without loss of generality, that p satisfies the following conditions:

1. p contains $s_i \cup s_j$ and $p \cap \mathcal{D}_{d,0}$ (resp. $p \cap \mathcal{D}_{d,\pm 1}$) consists only of unit squares whose color matches $\mathrm{color}(s_j)$ (resp. $\mathrm{color}(s_i)$).

2. p contains a square in $\{s_{j+1}, s_{j+2}, \ldots, s_{l-1}\}$ (resp. $\{s_{i+1}, s_{i+2} \ldots, s_{k-1}\}$) if $\mathrm{color}(s_k) = \mathrm{color}(s_j)$ and $l - j \geq 3$ (resp. $k - i \geq 3$).

3. p contains a square in $\{s_1, s_2 \ldots, s_{i-1}\}$ if $\mathrm{color}(s_k) \neq \mathrm{color}(s_j)$ and $i > 2$.

4. p contains $s_{|\mathcal{D}|}$ if $\mathrm{color}(s_k) \neq \mathrm{color}(s_j)$ and $i = 2$.

Consider the plug $\hat{p} = p \cup d$. By construction,

$$\mathbf{t}_{d,p} \sim \mathbf{t}_p^{-1} * (p, \varnothing, p^{-1}) * (p^{-1}, \varnothing, p) * f * f_{\mathrm{vert}} * (\hat{p}, \varnothing, \hat{p}^{-1}) * (\hat{p}^{-1}, \varnothing, \hat{p}) * \mathbf{t}_{\hat{p}}$$

where $f = (p, d, \hat{p}^{-1})$ and $f_{\mathrm{vert}} = (\hat{p}^{-1}, \varnothing, \hat{p})$. Thus, $\mathbf{t}_{d,p}$ contains four vertical dominoes in $\tilde{d} \times [|p|+1, |p|+5]$. Perform three flips (Figure 6.6 shows these flips for a specific hamiltonian disk) to conclude that

$$\mathbf{t}_{d,p} \sim \ldots * (p^{-1}, \tilde{d}, p \smallsetminus \tilde{d}) * (p \smallsetminus \tilde{d}, d, (\hat{p} \smallsetminus \tilde{d})^{-1}) * ((\hat{p} \smallsetminus \tilde{d})^{-1}, \varnothing, \hat{p} \smallsetminus \tilde{d}) * ((\hat{p} \smallsetminus \tilde{d}, \tilde{d}, (\hat{p} \smallsetminus \tilde{d})^{-1}) * \ldots$$

Then, it follows from Fact 2.3 that $\mathbf{t}_{d,p} \sim \mathbf{t}^{-1}_{\tilde{d}, p \smallsetminus \tilde{d}} * \mathbf{t}_{d, p \smallsetminus \tilde{d}} * \mathbf{t}_{\tilde{d}, \hat{p} \smallsetminus \tilde{d}}$.

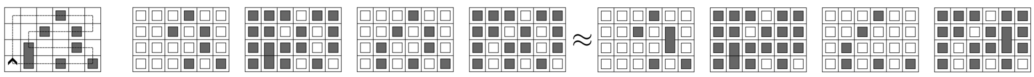

Figure 6.6: A domino d and a plug p in a hamiltonian disk, and the effect of thee flips in the tiling described by $(p^{-1}, \varnothing, p) * f * f_{\mathrm{vert}} * (p \cup d, \varnothing, (p \cup d)^{-1})$.

A careful analysis shows that under the four conditions above we have $\max\{|\operatorname{flux}_0(d, p \smallsetminus \tilde{d})|, |\operatorname{flux}_0(\tilde{d}, \hat{p} \smallsetminus \tilde{d})|, |\operatorname{flux}_0(\tilde{d}, p \smallsetminus \tilde{d})|\} < |\operatorname{flux}_0(d,p)|$. In the case where $\mathrm{color}(s_j) \neq \mathrm{sign}(\operatorname{flux}_0(d,p))$ we derive similar conditions that p must satisfy. As a consequence, we have that $\mathbf{t}_{d,p} \sim \mathbf{t}_{\tilde{d},p} * \mathbf{t}_{d, p \cup \tilde{d}} * \mathbf{t}^{-1}_{\tilde{d}, p \cup d}$ and $\max\{|\operatorname{flux}_0(d, p \cup \tilde{d})|, |\operatorname{flux}_0(\tilde{d}, p \cup d)|, |\operatorname{flux}_0(\tilde{d}, p)|\} < |\operatorname{flux}_0(d,p)|$. ■

We now focus on tilings $\mathbf{t}_{d,p}$ where $|\operatorname{flux}_0(d,p)| = 1$. The objective is to demonstrate that for any two such tilings $\mathbf{t}_{d,p}$ and $\mathbf{t}_{\tilde{d},\tilde{p}}$, we have $\mathbf{t}_{d,p} \sim \mathbf{t}^{\pm 1}_{\tilde{d},\tilde{p}}$. To this end, we first establish a partial result in this direction.

Lemma 6.6. *Let $\mathcal{D}$ be a disk with a hamiltonian cycle $\gamma = (s_1, s_2 \ldots, s_{|\mathcal{D}|})$ starting at $s_1 = s_{SW}$. Consider a domino $\tilde{d} \in \mathcal{D}_\gamma$ and a plug $\tilde{p} \in \mathcal{P}_d$ such that $|\operatorname{flux}_0(\tilde{d}, \tilde{p})| = 1$. Then, for each $d \in \mathcal{D}_\gamma$ there exists $p \in \mathcal{P}_d$ such that $|\operatorname{flux}_0(d,p)| = 1$ and $\mathbf{t}^{\pm 1}_{d,p} \sim \mathbf{t}_{\tilde{d},\tilde{p}}$.*

Proof. Take the sequence of dominoes $d_1, d_2, \ldots, d_n$ as in Lemma 6.2, so that $d_1 = \tilde{d}$ and $d_n = d$. We claim that there exist plugs $p_1, p_2, \ldots, p_n \in \mathcal{P}$ such that $p_1 = \tilde{p}$, $|\operatorname{flux}_0(d_{i+1}, p_{i+1})| = |\operatorname{flux}_0(d_i, p_i)|$ and $\mathbf{t}_{d_{i+1},p_{i+1}} \sim \mathbf{t}^{\pm 1}_{d_i,p_i}$. Notice that the claim implies the desired result.

From now on, we use Lemma 6.4 repeatedly without further mention. By construction, there are three possible relative positions of d_i and d_{i+1}. To prove the claim, we examine each case separately. First, suppose that $d_{i+1} = s_k \cup s_l$ with $s_k \subset \mathcal{D}_{d_i,0}$ and $s_l \subset \mathcal{D}_{d_i,\pm 1}$. Since $|\operatorname{flux}_0(d_i, p_i)| = 1$, we may assume that either $p_i = d_{i+1}$ or $p_i^{-1} = d_i \cup d_{i+1}$. If $p_i = d_{i+1}$ then, as in the proof of Lemma 6.5, $\mathbf{t}_{d_i,p_i} \sim \mathbf{t}^{-1}_{d_{i+1},\mathbf{p}_\circ} * \mathbf{t}_{d_i,\mathbf{p}_\circ} * \mathbf{t}_{d_{i+1},d_i}$. Thus, by Lemma 6.3, $\mathbf{t}_{d_i,p_i} \sim \mathbf{t}_{d_{i+1},d_i}$. For $p_i^{-1} = d_i \cup d_{i+1}$, we similarly have that $\mathbf{t}_{d_i,p_i} \sim \mathbf{t}_{d_{i+1},\mathbf{p}_\bullet \smallsetminus (d_i \cup d_{i+1})} * \mathbf{t}_{d_i,\mathbf{p}_\bullet \smallsetminus d_i} * \mathbf{t}^{-1}_{d_{i+1},\mathbf{p}_\bullet \smallsetminus d_{i+1}} \sim \mathbf{t}_{d_{i+1},\mathbf{p}_\bullet \smallsetminus (d_i \cup d_{i+1})}$. Therefore, in both cases, we obtain a plug p_{i+1} such that $|\operatorname{flux}_0(d_{i+1}, p_{i+1})| = |\operatorname{flux}_0(d_i, p_i)|$ and $\mathbf{t}_{d_i,p_i} \sim \mathbf{t}_{d_{i+1},p_{i+1}}$.

Secondly, suppose that $\mathcal{D}_{d_i,0} \smallsetminus \mathcal{D}_{d_{i+1},0}$ is a disk and $d_{i+1} = s_k \cup s_l$ with $s_k, s_l \subset \mathcal{D}_{d_i,0}$. Then, $\mathcal{D}_i = (\mathcal{D}_{d_i,0} \cup d_i) \smallsetminus \mathcal{D}_{d_{i+1},0}$ is also a disk and has a hamiltonian cycle γ_i induced by γ. Let $\gamma_{i,1}$ and $\gamma_{i,2}$ be the paths obtained from γ_i by disconnecting the adjacent unit squares in d_i and d_{i+1}. There are two cases: $|\gamma_{i,1}|$ and $|\gamma_{i,2}|$ are both either even or odd.

We obtain two tilings $\mathbf{t}_{i,1} \in \mathcal{T}(\mathcal{D}_i \times [0,1])$ and $\mathbf{t}_{i,2} \in \mathcal{T}((\mathcal{D}_i \smallsetminus d_i) \times [0,1])$ by placing dominoes along $\gamma_{i,1}$ and $\gamma_{i,2}$; Figure 6.7 illustrates an example of this construction. If $|\gamma_{i,1}|$ and $|\gamma_{i,2}|$ are even then $(d_i \cup d_{i+1}) \times [0,1] \notin \mathbf{t}_{i,1}$ and $d_{i+1} \times [0,1] \in \mathbf{t}_{i,2}$. If $|\gamma_{i,1}|$ and $|\gamma_{i,2}|$ are odd then $d_i \times [0,1] \notin \mathbf{t}_{i,1}$, $d_{i+1} \times [0,1] \in \mathbf{t}_{i,1}$ and $d_{i+1} \times [0,1] \notin \mathbf{t}_{i,2}$. Let $f^*_{i,1}$ and $f^*_{i,2}$ be the set of planar dominoes that describes $\mathbf{t}_{i,1}$ and $\mathbf{t}_{i,2}$, respectively.

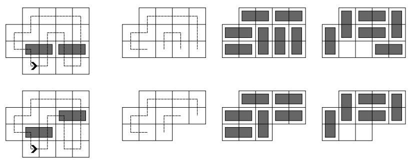

Figure 6.7: Two examples of a disk with a hamiltonian cycle γ and dominoes d_i and d_{i+1}, the disk $\mathcal{D}_i$ with paths $\gamma_{i,1}$ and $\gamma_{i,2}$, and the tilings $\mathbf{t}_{i,1}$ and $\mathbf{t}_{i,2}$. In the first (resp. second) example $|\gamma_{i,1}|$ and $|\gamma_{i,2}|$ are both even (resp. odd).

Consider the tiling $\mathbf{t}_{d_i,p_i} = \mathbf{t}^{-1}_{p_i} * f * f_{\text{vert}} * \mathbf{t}_{p_i \cup d_i}$. Since $|\operatorname{flux}_0(d_i, p_i)| = 1$, we may assume that $p_i \cap \mathcal{D}_{d_i,0} \subset \mathcal{D}_{d_{i+1},0}$. Then, $\mathbf{t}_{d_i,p_i}$ covers the region $(\mathcal{D}_{d_i,0} \smallsetminus \mathcal{D}_{d_{i+1},0}) \times [|p_i|, |p_i| + 2]$ only with vertical dominoes. Since $\mathcal{D}_i$ is a disk, as in the proof of Lemma 6.3, we have a sequence of flips that takes $\mathbf{t}_{d_i,p_i}$ to the tiling $\mathbf{t} = \mathbf{t}^{-1}_{p_i} * (p_i, f^*_{i,1}, (\mathcal{D}_i \cup p_i)^{-1}) * ((\mathcal{D}_i \cup p_i)^{-1}, f^*_{i,2}, p_i \cup d_i) * \mathbf{t}_{p_i \cup d_i}$. From Facts 2.3 and 2.4, if $|\gamma_{i,1}|$ and $|\gamma_{i,2}|$ are odd (resp. even) then $\mathbf{t}$ is $\sim$-equivalent to $\mathbf{t}_{d_{i+1},p_i}$ (resp. $\mathbf{t}^{-1}_{d_{i+1},p_i \cup d_i}$). Thus, in any case, we have a plug p_{i+1} such that $\mathbf{t}_{d_i,p_i} \sim \mathbf{t}^{\pm 1}_{d_{i+1},p_{i+1}}$ and $\operatorname{flux}_0(d_{i+1}, p_{i+1}) = \operatorname{flux}_0(d_i, p_i)$. Finally, notice that a completely analogous argument holds in the third possible case, when $d_{i+1} = s_k \cup s_l$ with $s_k, s_l \subset \mathcal{D}_{d_i,\pm 1}$ and $\mathcal{D}_{d_i,\pm 1} \smallsetminus \mathcal{D}_{d_{i+1},\pm 1}$ is a disk. ∎

For hamiltonian disks without bottlenecks, we now demonstrate the existence of a domino that, in a certain sense, connects the family of tilings with flux equals $+1$ to the family of tilings with flux equals -1. As a corollary, we conclude that the even domino group of a bottleneck-free hamiltonian disk is cyclic.

Lemma 6.7. *Let $\mathcal{D}$ be a nontrivial quadriculated disk with a hamiltonian cycle $\gamma = (s_1, s_2 \ldots, s_{|\mathcal{D}|})$ starting at $s_1 = s_{SW}$. If no domino disconnects $\mathcal{D}$ then there exist a domino $d \in \mathcal{D}_\gamma$ such that $\mathbf{t}_{d,p}^{-1} \sim \mathbf{t}_{d,p^{-1}\smallsetminus d}$ for every plug $p \in \mathcal{P}_d$ with* $\operatorname{flux}_0(d,p) = 1$.

Proof. Notice that s_1 is contained in a 3×3 square $\widetilde{\mathcal{D}}$, as no domino disconnects $\mathcal{D}$ and $s_1 = s_{SW}$. Suppose that in $\widetilde{\mathcal{D}}$ the cycle γ follows one of the three patterns illustrated in Figure 6.8; the other cases are obtained by reversing the orientation, and the argument proceeds similarly. We say that γ is of type i if it follows the i-th possible pattern.

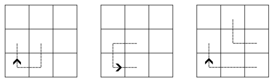

Figure 6.8: Three possible patterns of γ in $\widetilde{\mathcal{D}}$.

Let d be the domino adjacent and parallel to $s_1 \cup s_{|\mathcal{D}|}$. Suppose that γ is either of type 1 or type 3; the case where γ is of type 2 is analogous to the case where γ is of type 1. Consider a plug $p \in \mathcal{P}_d$ such that $\operatorname{flux}_0(d,p) = 1$. Then, it follows that $\operatorname{flux}_0(d, p^{-1} \smallsetminus d) = -1$. By Lemma 6.4, it suffices to consider the case in which $p^{-1} \smallsetminus d = s_{|\mathcal{D}|} \cup s_i$, where $s_i \subset \widetilde{\mathcal{D}} \smallsetminus d$ denotes the unit square adjacent to s_2.

Consider the tiling $\mathbf{t}_{d,p^{-1}\smallsetminus d} = \mathbf{t}_{p^{-1}\smallsetminus d}^{-1} * f * f_{\text{vert}} * \mathbf{t}_{p^{-1}}$. Insert vertical floors around f and f_{vert} to obtain a tiling $\mathbf{t}_1 \sim \mathbf{t}_{d,p^{-1}\smallsetminus d}$; the restriction of $\mathbf{t}_1$ to $\widetilde{\mathcal{D}} \times [|p^{-1} \smallsetminus d|, |p^{-1} \smallsetminus d| + 7]$ is shown in the first row of Figure 6.9. Let $\mathbf{t}_i$ be the tiling whose restriction to $\widetilde{\mathcal{D}} \times [|p^{-1} \smallsetminus d|, |p^{-1} \smallsetminus d| + 7]$ is as in the i-th first row of Figure 6.9 and which is equal to $\mathbf{t}_1$ outside this region. We have $\mathbf{t}_1 \approx \mathbf{t}_2$ and $\mathbf{t}_3 \approx \mathbf{t}_4 \approx \mathbf{t}_5$. Notice that the restrictions of $\mathbf{t}_2$ and $\mathbf{t}_3$ to $\widetilde{\mathcal{D}} \times [|p^{-1} \smallsetminus d| + 2, |p^{-1} \smallsetminus d| + 6]$ define two tilings, both with the same twist, of a $3 \times 3 \times 4$ box. Since the 3×4 rectangle is regular (see Lemma 9.2 of [22]), it follows that $\mathbf{t}_2 \sim \mathbf{t}_3$.

We focus on $\mathbf{t}_4$ when γ is of type 1. Let $f_1, f_2, \ldots, f_7$ be the seven floors of $\mathbf{t}_4$ whose restriction is shown in Figure 6.9. By Facts 2.1 and 2.3, we have $\mathbf{t}_4 \sim \mathbf{t}_{f_2^{-1}}^{-1} * \mathbf{t}_{f_3} * \mathbf{t}_{f_4^{-1}}^{-1} * \mathbf{t}_{f_6^{-1}}^{-1} * \mathbf{t}_{f_7}$, since all other floors of $\mathbf{t}_4$ contains only

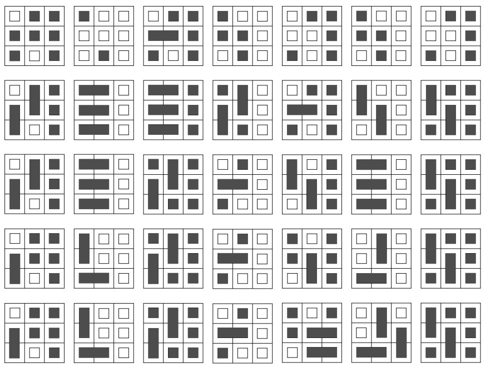

Figure 6.9: The i-th row shows the restriction to $\widetilde{\mathcal{D}}$ of seven floors of a tiling $\mathbf{t}_i$.

dominoes that respect γ. Now, it follows from Fact 2.4 and Lemma 6.3 that $\mathbf{t}_4 \sim \mathbf{t}_{f_4^{-1}}^{-1}$. On the other hand, $\mathbf{t}_{f_4^{-1}}^{-1} = \mathbf{t}_{d,s_1 \cup s_j}^{-1}$, where $s_j \subset \widetilde{\mathcal{D}} \setminus s_2$ is the unit square adjacent to s_i. Finally, by Lemma 6.4, $\mathbf{t}_{d,s_1 \cup s_j}^{-1} \sim \mathbf{t}_{d,p}^{-1}$. Similarly, when γ is of type 3, we have $\mathbf{t}_5 \sim \mathbf{t}_{d,p}^{-1}$. ■

Corollary 6.8. *Let $\mathcal{D}$ be a nontrivial hamiltonian balanced quadriculated disk. Suppose that no domino disconnects $\mathcal{D}$. If $d_1, d_2 \in \mathcal{D}_\gamma$ and $p_1, p_2 \in \mathcal{P}$ are such that $|\operatorname{flux}_0(d_1, p_1)| = 1 = |\operatorname{flux}_0(d_2, p_2)|$ then $\mathbf{t}_{d_1,p_1}^{\pm 1} \sim \mathbf{t}_{d_2,p_2}$.*

Proof. Take the domino d as in Lemma 6.7. By Lemma 6.6, there are plugs p and $\tilde{p}$ with $|\operatorname{flux}_0(d,p)| = 1 = |\operatorname{flux}_0(d,\tilde{p})|$ such that $\mathbf{t}_{d_1,p_1}^{\pm 1} \sim \mathbf{t}_{d,p}$ and $\mathbf{t}_{d_2,p_2}^{\pm 1} \sim \mathbf{t}_{d,\tilde{p}}$. The result now follows from an application of Lemma 6.4. Indeed, we have either $\mathbf{t}_{d,p} \sim \mathbf{t}_{d,\tilde{p}}$ or $\mathbf{t}_{d,p} \sim \mathbf{t}_{d,p^{-1} \setminus d}^{-1} \sim \mathbf{t}_{d,\tilde{p}}^{-1}$, depending on whether $\operatorname{flux}_0(d,p) = \operatorname{flux}_0(d,\tilde{p})$ or $\operatorname{flux}_0(d,p) = -\operatorname{flux}_0(d,\tilde{p})$. ■

The proof of Theorem 1.6 follows directly from the established results.

Proof of Theorem 1.6. Since $\mathcal{D}$ is nontrivial, by Fact 2.7, the twist $\operatorname{Tw}\colon G_{\mathcal{D}}^{+} \to \mathbb{Z}$ is a surjective homomorphism. It follows from Lemma 6.5 and Corollary 6.8 that $G_{\mathcal{D}}^{+}$ is cyclic. Consequently, the twist is an isomorphism. ■

Our approach to prove Theorem 1.7 is based on utilizing the established regularity of bottleneck-free hamiltonian disks. We need an additional lemma concerning generators $\mathbf{t}_{d,p}$ in the case where $\mathcal{D} \setminus d$ is not connected.

Lemma 6.9. *Consider a disk $\mathcal{D}$ satisfying the hypothesis of Theorem 1.7. Let $d \in \mathcal{D}_\gamma$ be a domino that disconnects $\mathcal{D}$ and consider a plug $p \in \mathcal{P}_d$. Then, $\mathbf{t}_{d,p}$ is $\sim$-equivalent to a concatenation of tilings $\mathbf{t}_{\tilde{d},\tilde{p}}^{\pm 1}$ with $\mathcal{D} \setminus \tilde{d}$ connected.*

Proof. We first distinguish four planar dominoes. Suppose that $d \subset \mathcal{D}_i$ for some $i > 0$, otherwise set $d_1 = d$. Let $d_1 \subset \mathcal{D}_0$ be the domino that contains the line segment of length two defined by $\mathcal{D}_0$ and $\mathcal{D}_i$. Thus, $\mathcal{D} \setminus d_1$ is not connected. Let $d_2 \subset \mathcal{D}_0$ be the domino adjacent and parallel to d_1 and denote by d_3 and d_4 the dominoes obtained after performing a flip on d_1 and d_2. Notice that $\mathcal{D} \setminus d_2$ is connected, and at least one of the regions $\mathcal{D} \setminus d_3$ or $\mathcal{D} \setminus d_4$ is also connected.

Assume, without loss of generality, that the initial unit square of the hamiltonian cycle of $\mathcal{D}$ is contained in $\mathcal{D}_0$. Then, we have $\mathcal{D}_{d_1,0} = \mathcal{D}_i$. Notice that $\mathcal{D}_{d_1,0} \smallsetminus \mathcal{D}_{d,0}$ is a hamiltonian disk, as d and d_1 disconnect $\mathcal{D}$. Since $|\mathcal{D}_i| < |\mathcal{D}_0| - 2$, we can modify p to obtain a plug p_1 such that $p_1 \subset \mathcal{D}_{d,0} \cup \mathcal{D}_0 \smallsetminus d_1$, $d_2 \subset p_1^{-1}$ and $\operatorname{flux}_0(d,p) = \operatorname{flux}_0(d,p_1)$. For an example of this construction, see Figure 6.10. It follows from Lemma 6.4 that $\mathbf{t}_{d,p} \sim \mathbf{t}_{d,p_1}$. Furthermore, as in the proof of Lemma 6.3, we have $\mathbf{t}_{d,p_1} \sim \mathbf{t}_{d_1,p_1}^{\pm 1}$.

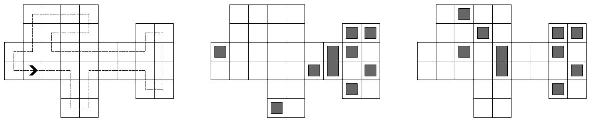

Figure 6.10: A hamiltonian disk $\mathcal{D}$ where $\mathcal{D}_0$ is equal to a 4×4 square, a domino d with a compatible plug p, and the domino d_1 with a plug p_1.

Since $d_2 \subset p_1^{-1}$, a vertical flip modifies $\mathbf{t}_{d_1,p_1}$ to now contain the dominoes $d_2 \times [K, K+1]$ and $d_2 \times [K+1, K+2]$, where $K = |p_1|$. A horizontal flip then takes $d_1 \times [K, K+1]$ and $d_2 \times [K, K+1]$ to $d_3 \times [K, K+1]$ and $d_4 \times [K, K+1]$. Thus, Facts 2.3 and 2.4 imply that $\mathbf{t}_{d_1,p} \sim \mathbf{t}_{d_3,p} * \mathbf{t}_{d_4,p\cup d_3} * \mathbf{t}_{d_2,p\cup d_1}^{-1}$.

Therefore, the tiling $\mathbf{t}_{d,p}$ is $\sim$-equivalent to a concatenation of tilings of the form $\mathbf{t}_{\tilde{d},\tilde{p}}^{\pm 1}$. By Fact 2.1, we have $\mathbf{t}_{\tilde{d},\tilde{p}}^{\pm 1} \sim \mathbf{t}_{\mathrm{vert}}$ if $\tilde{d} \notin \mathcal{D}_\gamma$. Otherwise, by construction, $\tilde{d}$ is either a domino that does not disconnect $\mathcal{D}$ or satisfies $\operatorname{flux}_0(\tilde{d},\tilde{p}) = 0$. The result then follows from Lemma 6.3. ■

We are now ready to prove Theorem 1.7.

Proof of Theorem 1.7. Lemmas 6.5, 6.6 and 6.9 imply that the even domino group $G_{\mathcal{D}}^{+}$ is generated by tilings $\mathbf{t}_{d,p}$ with $d \subset \mathcal{D}_0$ and $p \in \mathcal{P}_d$ such that $\mathcal{D} \smallsetminus d$ is connected and $|\operatorname{flux}_0(d,p)| = 1$. By Lemma 6.4, we may further restrict to plugs contained in $\mathcal{D}_0$. We claim that each such tiling $\mathbf{t}_{d,p}$ is equivalent under $\sim$ to a tiling of $\mathcal{D} \times [0, 2N]$ whose restriction to $(\mathcal{D} \smallsetminus \mathcal{D}_0) \times [0, 2N]$ is composed solely of vertical dominoes. Notice that the desired result follows from the claim, since $\mathcal{D}_0$ is regular by Theorem 1.6.

The hamiltonian cycle γ of $\mathcal{D}$ induces a hamiltonian cycle γ_0 in $\mathcal{D}_0$. The dominoes that respect γ_0 but do not respect γ are exactly the dominoes $d_i \subset \mathcal{D}_0$ that contain the line segment defined by $\mathcal{D}_0$ and $\mathcal{D}_i$. Let $\mathbf{t}$ be the tiling of $\mathcal{D} \times [0, 2N]$ obtained from the tiling $\mathbf{t}_{d,p;\gamma_0}$ of $\mathcal{D}_0 \times [0, 2N]$ by covering the region $(\mathcal{D} \smallsetminus \mathcal{D}_0) \times [0, 2N]$ with vertical dominoes. It follows from Facts 2.3 and 2.4 that $\mathbf{t}$ is $\sim$-equivalent to a concatenation of $\mathbf{t}_{d,p;\gamma}$ and possibly tilings $\mathbf{t}_{d_i,p_i;\gamma}^{\pm 1}$ such that $\operatorname{flux}_0(d_i, p_i) = 0$. Thus, by Lemma 6.3, we have $\mathbf{t} \sim \mathbf{t}_{d,p;\gamma}$ and the claim follows. ■

7
References

[1] ANGEL, O.; RICHEY, J.; SPINKA, Y. ; YEHUDAYOFF, A.. **Random walks on regular trees can not be slowed down**. Electronic Journal of Probability, 29:1–15, 2024.

[2] BEDNIK, G.. **Hopfions in a lattice dimer model**. Physical Review B, 100(2):024420, 2019.

[3] CHANDGOTIA, N.; SHEFFIELD, S. ; WOLFRAM, C.. **Large deviations for the 3d dimer model**. arXiv preprint arXiv:2304.08468, 2023.

[4] COHN, H.; ELKIES, N. ; PROPP, J.. **Local statistics for random domino tilings of the aztec diamond**. Duke Math. J., 85(1):117–166, 1996.

[5] COHN, H.; KENYON, R. ; PROPP, J.. **A variational principle for domino tilings**. Journal of the American Mathematical Society, 14(2):297–346, 2001.

[6] CONWAY, J. H.; LAGARIAS, J. C.. **Tiling with polyominoes and combinatorial group theory**. Journal of combinatorial theory, Series A, 53(2):183–208, 1990.

[7] FREEDMAN, M.; HASTINGS, M. B.; NAYAK, C. ; QI, X.-L.. **Weakly coupled non-abelian anyons in three dimensions**. Physical Review B—Condensed Matter and Materials Physics, 84(24):245119, 2011.

[8] FREIRE, J.; KLIVANS, C.; MILET, P. ; SALDANHA, N.. **On the connectivity of spaces of three-dimensional domino tilings**. Transactions of the American Mathematical Society, 375(3):1579–1605, 2022.

[9] JOCKUSCH, W.; PROPP, J. ; SHOR, P.. **Random domino tilings and the arctic circle theorem**. arXiv preprint arXiv:9801068, 1995.

[10] KASTELEYN, P. W.. **The statistics of dimers on a lattice: I. the number of dimer arrangements on a quadratic lattice**. Physica, 27(12):1209–1225, 1961.

[11] KESHAVARZ-KOHJERDI, F.; BAGHERI, A.. **Finding hamiltonian cycles of truncated rectangular grid graphs in linear time**. Applied Mathematics and Computation, 436:127513, 2023.

[12] KHESIN, B.; SALDANHA, N. C.. **Relative helicity and tiling twist**. arXiv preprint arXiv:2408.00522, 2024.

[13] KLIVANS, C. J.; SALDANHA, N. C.. **Domino tilings and flips in dimensions 4 and higher**. Algebraic Combinatorics, 5(1):163–185, 2022.

[14] LYONS, R.; PERES, Y.. **Probability on trees and networks**, volumen 42. Cambridge University Press, 2017.

[15] DE MARREIROS, R.. **3D domino tilings: irregular disks and connected components under flips**. arXiv preprint arXiv:2209.03109, 2022.

[16] DE MARREIROS, R.. **Domino tilings of 3D cylinders and regularity of disks**. Master dissertation `https://doi.org/10.17771/PUCRio.acad.53188`, 2021.

[17] DE MARREIROS, R.. **Domino tilings of three-dimensional cylinders: regularity of hamiltonian disks**. arXiv preprint arXiv:2406.11777, 2024.

[18] MILET, P. H.; SALDANHA, N. C.. **Domino tilings of three-dimensional regions: flips and twists**. arXiv preprint arXiv:1410.7693, 2018.

[19] MILET, P. H.; SALDANHA, N. C.. **Flip invariance for domino tilings of three-dimensional regions with two floors**. Discrete & Computational Geometry, 53:914–940, 2015.

[20] PAK, I.; YANG, J.. **The complexity of generalized domino tilings**. The Electronic Journal of Combinatorics, p. P12–P12, 2013.

[21] SALDANHA, N. C.. **Domino tilings of cylinders: Connected components under flips and normal distribution of the twist**. The Electronic Journal of Combinatorics, p. P1–28, 2021.

[22] SALDANHA, N. C.. **Domino tilings of cylinders: the domino group and connected components under flips**. Indiana Univ. Math. J., 71(3):965–1002, 2022.

[23] SALDANHA, N. C.; TOMEI, C.; CASARIN, M. A. ; ROMUALDO, D.. **Spaces of domino tilings**. Discrete & Computational Geometry, 14:207–233, 1995.

[24] TEMPERLEY, H. N.; FISHER, M. E.. **Dimer problem in statistical mechanics-an exact result**. Philosophical Magazine, 6(68):1061–1063, 1961.

[25] THURSTON, W. P.. **Conway's tiling groups**. The American Mathematical Monthly, 97(8):757–773, 1990.

[26] ZAMFIRESCU, C.; ZAMFIRESCU, T.. **Hamiltonian properties of grid graphs**. SIAM Journal on Discrete Mathematics, 5(4):564–570, 1992.